Electronic Supporting Information

Enclosing Classical Polyoxometallates in Silver Nanoclusters

Zhi Wang,[a] Yi-Ming Sun,[a] Qing-Ping Qu,[a] Yu-Xin Liang,[a] Xing-Po Wang,*[,a] Qing-Yun Liu,[c] Mohamedally Kurmoo,[b] Hai-Feng Su,*[,d] Chen-Ho Tung,[a] and Di Sun*[,a]

[a]Key Lab of Colloid and Interface Chemistry, Ministry of Education, School of Chemistry and Chemical Engineering, Shandong University, Jinan, 250100, People's Republic of China

[b]Institut de Chimie de Strasbourg, Université de Strasbourg, CNRS-UMR 7177, 4 rue Blaise Pascal, 67008 Strasbourg Cedex, France

[c]College of Chemical and Environmental Engineering, Shandong University of Science and Technology, Qingdao, 266590, P. R. China.

[d]State Key Laboratory for Physical Chemistry of Solid Surfaces and Department of Chemistry, College of Chemistry and Chemical Engineering, Xiamen University, Xiamen, 361005, P. R. China.

Experimental details

The precursor $[Ag(EtS)]_n$ was synthesized via a literature procedure with some modification.[1] EtSH (Adamas-beta®) was purchased from Shanghai Titan Scientific Co.,Ltd. All other chemicals and solvents used in the syntheses were of analytical grade and used without further purification. IR spectra were recorded on a PerkinElmer Spectrum Two in the frequency range of 4000-500 cm^{-1}. The elemental analyses (C and H) were determined on a Vario EL III analyzer. The diffuse-reflectance spectra were recorded on a UV/Vis spectrophotometer (Evolution 220, ISA-220 accessory, Thermo Scientific) using a built-in 10 mm silicon photodiode with a 60 mm Spectralon sphere. Powder X-ray diffraction (PXRD) data were collected on a Philips X'Pert Pro MPD X-ray diffractometer with CuKα radiation equipped with an X'Celerator detector. Morphology of the samples and elemental composition analyses were measured using an SU-8010 field emission scanning electron microscope (FESEM; Hitachi Ltd., Tokyo, Japan) equipped with an Oxford-Horiba Inca XMax50 energy dispersive X-ray spectroscopy (EDS) attachment (Oxford Instruments Analytical, High Wycombe, England).

X-ray Crystallography

Single crystals of **SD/Ag44a**, **SD/Ag46** and **SD/Ag44b** with appropriate dimensions were chosen under an optical microscope and quickly coated with high vacuum grease (Dow Corning Corporation) to prevent decomposition. Crystal was mounted on CryoLoop™ loop and the cell parameters and intensity data were recorded on a Rigaku Oxford Diffraction XtaLAB Synergy-S diffractometer equipped with a HyPix-6000HE Hybrid Photon Counting (HPC) detector operating in shutterless mode and an Oxford Cryosystems Cryostream 800 Plus at 100 K using Mo Kα (λ = 0.71073 Å) for **SD/Ag44a** from PhotonJet micro-focus X-ray Source. Data were processed using the *CrystAlis*^{Pro} software suite.[2] Intensity data and cell parameters of **SD/Ag46** and **SD/Ag44b** were recorded at 123 K on a Bruker Apex II single crystal diffractometer, employing a Mo K_α radiation (λ = 0.71073 Å) and a CCD area detector. The raw frame data were processed using SAINT and SADABS to yield the reflection data file.[3] The structure was solved using the charge-flipping algorithm, as implemented in the program *SUPERFLIP*[4] and refined by full-matrix least-squares techniques against F_o^2 using the SHELXL program[5] through the OLEX2 interface.[6] Hydrogen atoms at carbon were placed in calculated positions and refined isotropically by using a riding model. Appropriate restraints or constraints were applied to the geometry and the atomic displacement parameters of the atoms in the cluster. All structures were examined using the Addsym subroutine of PLATON[7] to ensure that no additional symmetry could be applied to the models. Pertinent crystallographic data collection and refinement parameters are collated in Table S2. Selected bond lengths and angles are collated in Table S3.

Synthesis Details

Synthesis of $(EtSAg)_n$

The solution of $AgNO_3$ (30 mmol, 5 g) in 75 mL acetonitrile was mixed with 100 mL ethanol containing EtSH (30 mmol, 2.1 mL) and 5 mL Et_3N under stirring for 3 hours in the dark at room temperature, then the yellow powder of $(EtSAg)_n$ was isolated by filtration and washed with 10 mL ethanol and 20 mL ether, then dried in the ambient environment (yield: 95 %).

Synthesis of $[(V_{10}O_{28})@Ag_{44}(EtS)_{20}(PhSO_3)_{18}(H_2O)_2]_n$ (SD/Ag44a)

0.2 mL H_2O containing $PhSO_3H$ (0.15 mmol, 23.7 mg) was added into 5 mL *n*-butanol containing $(EtSAg)_n$ (0.05 mmol, 8.5 mg), Ag_2O (0.05 mmol, 11.6 mg) and $NaVO_3$ (0.04 mmol, 4.8 mg), the mixture was treated under KQ5200DE ultrasonic instrument (160 W, Kun Shan Ultrasonic Instruments Co.) for 15 minutes (as the ultrasound would produce considerable heat during the experiment, cleaning fluid water should be replaced every 5 min), then the reaction mixture was sealed and heated at 70 °C for 1200 min, after cooling to room temperature, the yellow solution was filtrated and evaporated in the dark for 1 month, red block crystals were obtained in a yield of 18 %. Elemental analyses calc. (found) for $C_{148}H_{194}Ag_{44}O_{84}S_{38}V_{10}$ (**SD/Ag44a**), calcd (found): C, 18.15 (18.09); H, 2.00 (1.97) %. IR: 2950 (w), 1441 (w), 1114 (s), 1029 (m), 1108 (s), 987 (s), 915 (m), 818 (w), 755 (m), 721 (s), 686 (s), 602 (s), 552 (s) cm^{-1}.

Synthesis of $[(V_{10}O_{28})@Ag_{46}(EtS)_{23}(PhSO_3)_{15}(CO_3)]_n$ (SD/Ag46)

The synthesis of **SD/Ag46** was similar to that of **SD/Ag44a** except for using methanol instead of *n*-butanol, after cooling to room temperature, red block crystals were isolated in a yield of 20 %. Elemental analyses calc. (found) for $C_{137}H_{190}Ag_{46}O_{76}S_{38}V_{10}$ (**SD/Ag46**), calcd (found): C, 16.89 (16.80); H, 1.97 (1.91) %. IR: 2942 (w), 1444 (m), 1258 (w), 1135 (m), 1119 (s), 1029 (m), 1007 (s), 992 (s), 993 (m), 788 (m), 755 (m), 721 (s), 691 (s), 602 (s), 557 (s) cm^{-1}.

Synthesis of $[(Mo_6O_{19})@Ag_{44}(EtS)_{24}(SCl_4)_3]_n$ (SD/Ag44b)

The mixture of $AgNO_3$ (0.1 mmol, 17 mg) and $(EtSAg)_n$ (0.05 mmol, 8.5 mg) were mixed in the mixed solution of methanol and acetonitrile (5 mL, v:v=1:1). The mixture was sonicated in a KQ5200DE ultrasonic instrument (160 W, Kun Shan Ultrasonic Instruments Co.) for 20 min (as the ultrasound would produce considerable heat during the experiment, cleaning fluid water should be replaced every 5 min). To this solution, $(NH_4)_6Mo_7O_{24}$ (0.005 mmol, 6.2 mg) and 2d TMEDA were added. The reaction continued for further 20 minutes under the same ultrasonic condition. The yellow turbid liquid was sealed and heated at 80 °C for 2000 minutes, after cooling to room temperature, **SD/Ag44b** was obtained in a yield of <5%. Elemental analyses calc. (found) for $C_{48}H_{120}Ag_{44}Cl_{12}Mo_6O_{19}S_{27}$ (**SD/Ag44b**), calcd (found): C, 7.57 (7.48); H, 1.59 (1.45) %.

Figure S1: The μ_4 coordination mode of EtS^- ligands towards silver shell in SD/Ag44a.

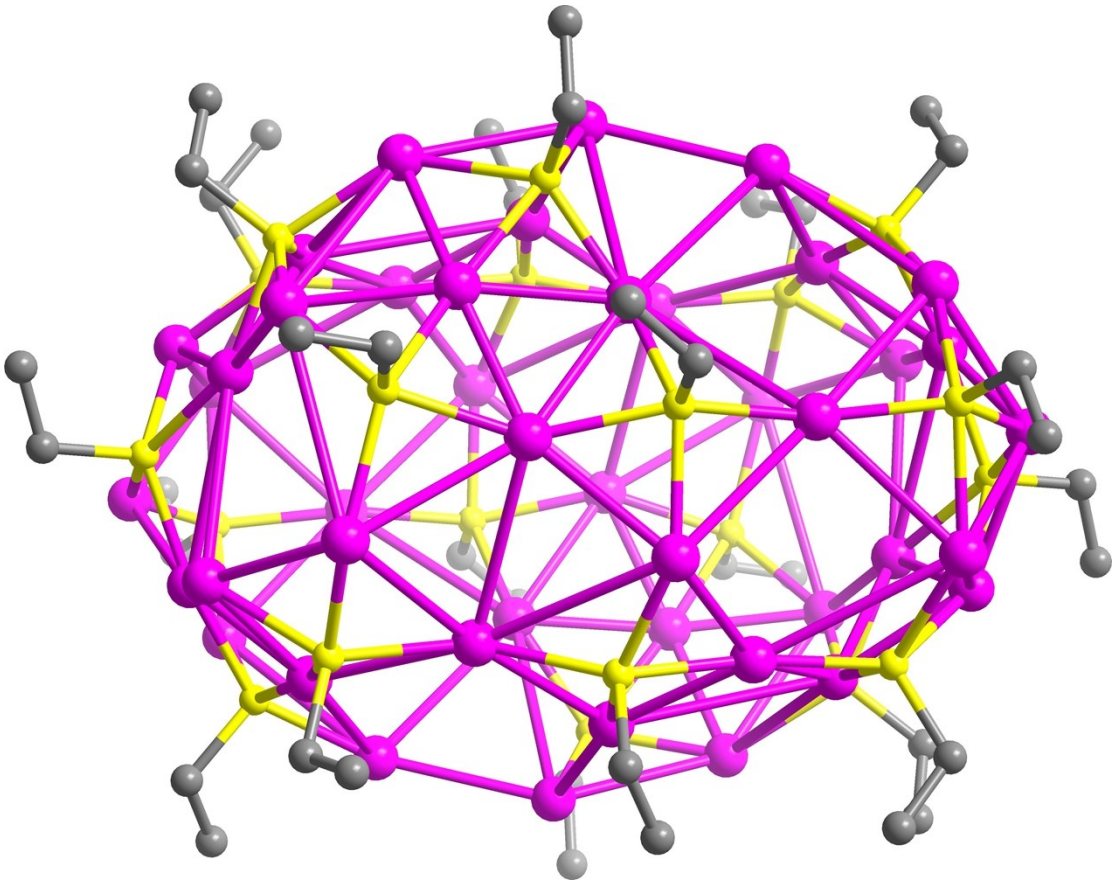

Figure S2: The $V_{10}O_{28}^{6-}$ encapsulated by Ag_{44} and Ag_{40} shells in SD/Ag44a (a) and reported Ag_{40} cluster[8] (b).

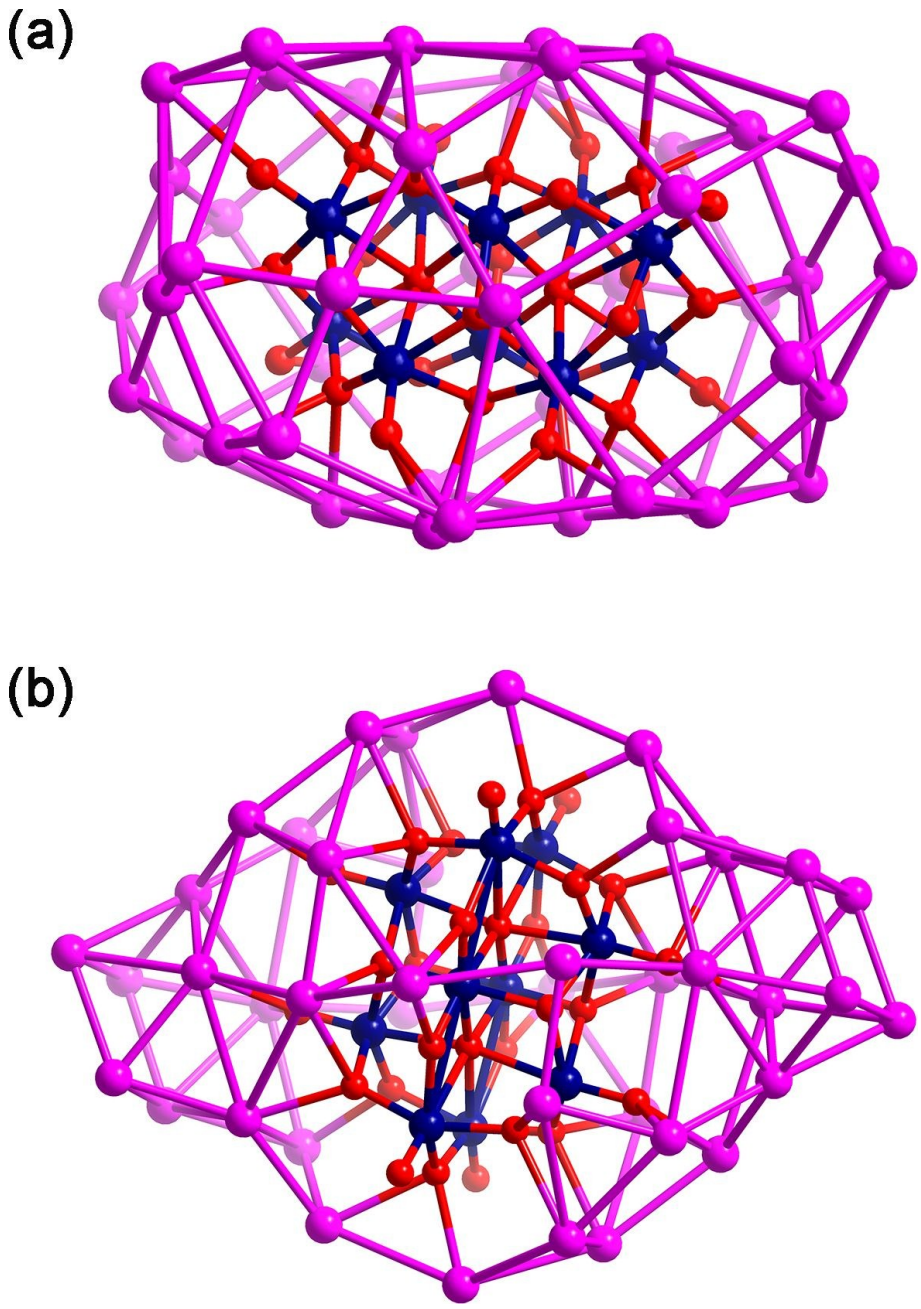

Figure S3: The binding mode of $V_{10}O_{28}^{6-}$ towards silver atoms in SD/Ag46.

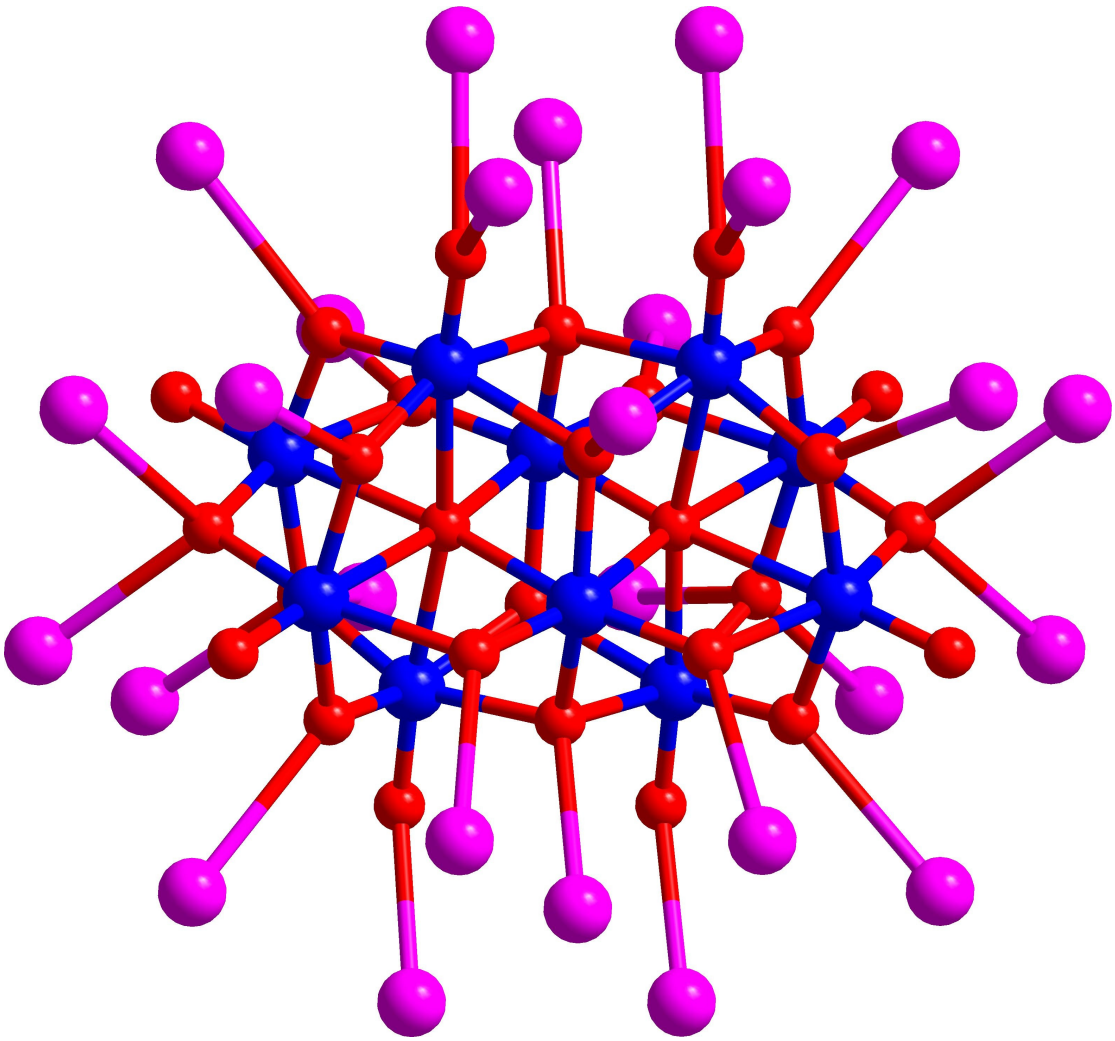

Figure S4: The binding mode of $Mo_6O_{19}^{2-}$ towards silver atoms in SD/Ag44b.

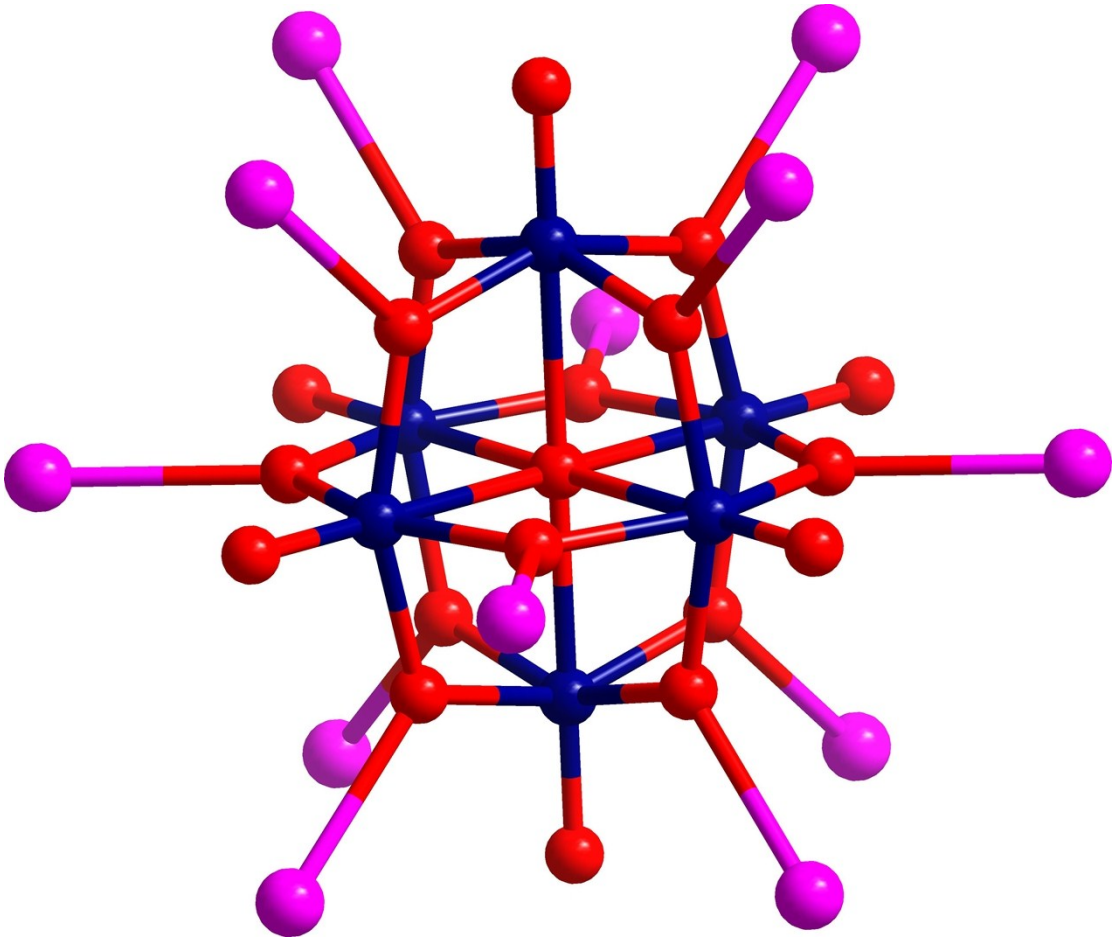

Figure S5: View of the 3D framework (a) and simplified primitive cubic (*pcu*) topology (b) with the Ag_{44} subunit as a node (highlighted in red ball) of SD/Ag44b.

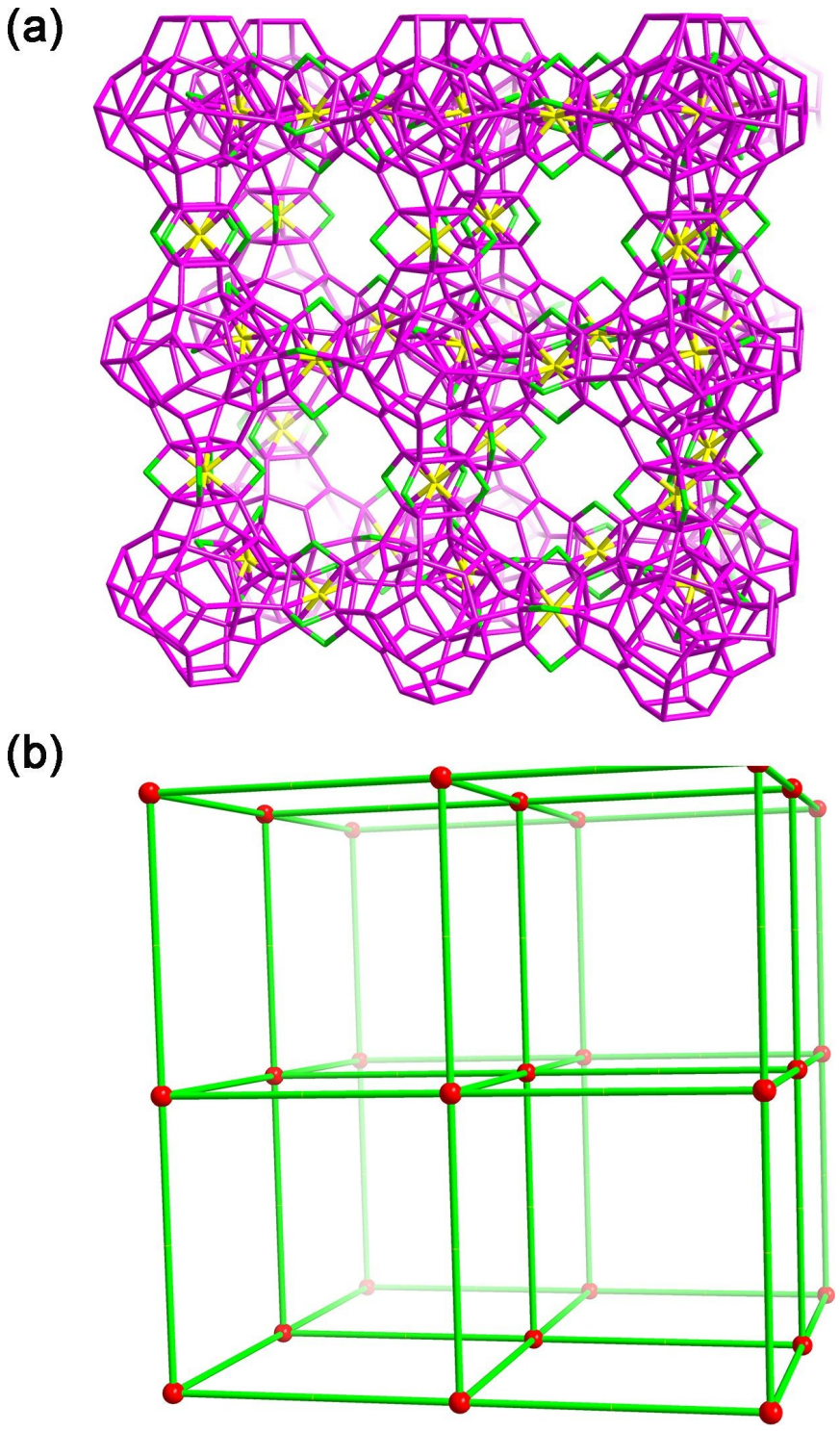

Figure S6: Plot of anodic currents versus the square root of the scan rate for SD/Ag46-CPE.

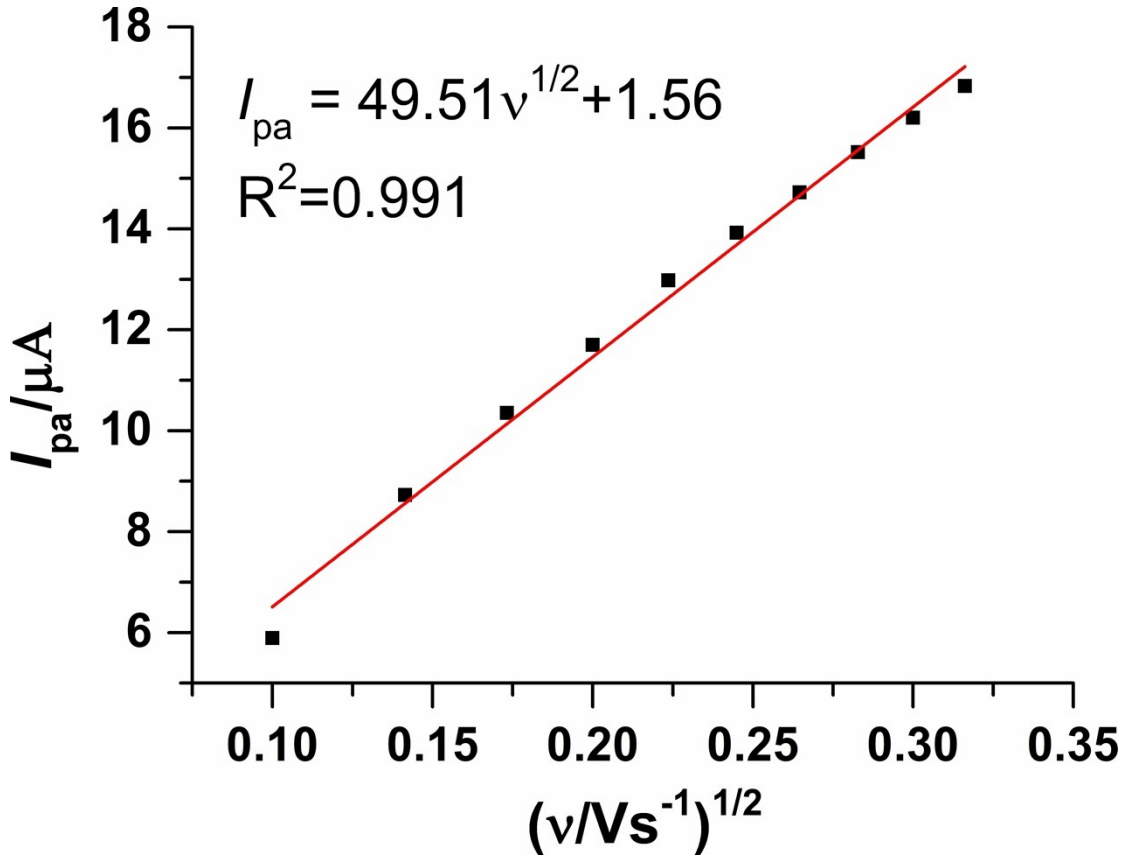

Figure S7: Compared PXRD patterns of SD/Ag44a.

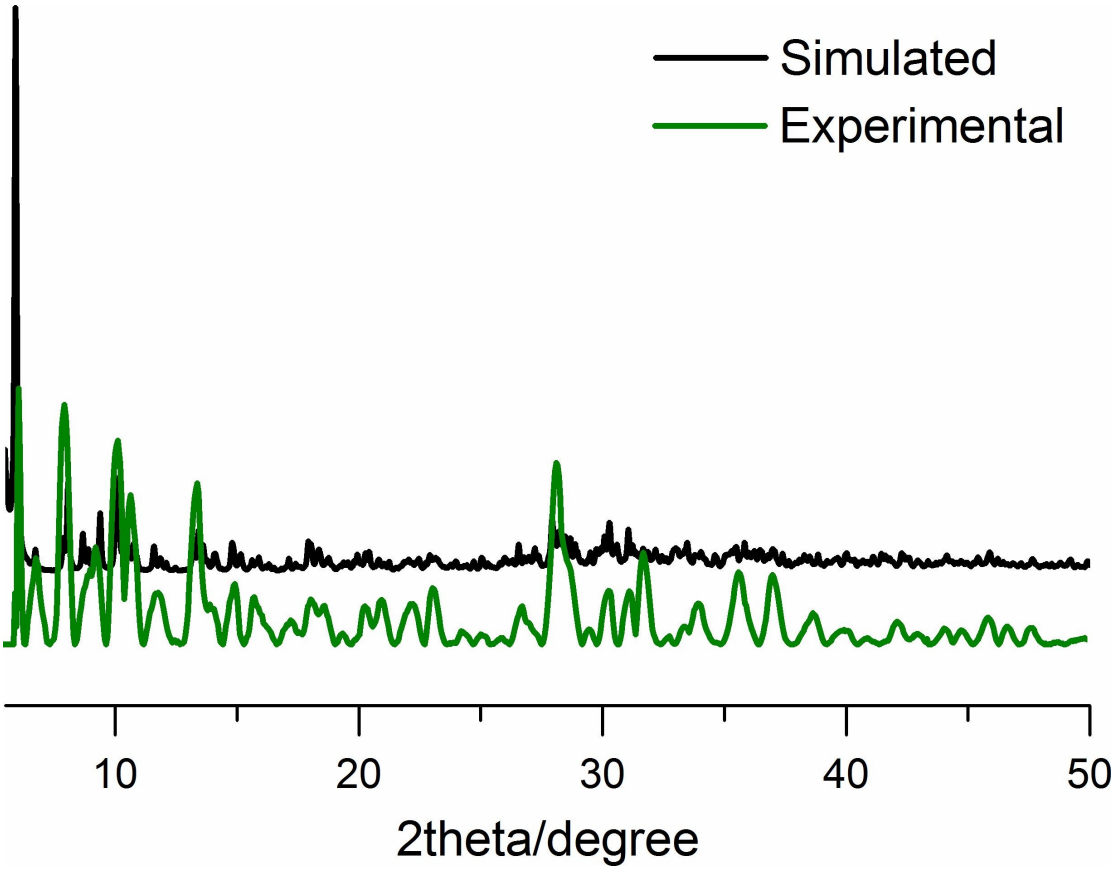

Figure S8: Compared PXRD patterns of SD/Ag46.

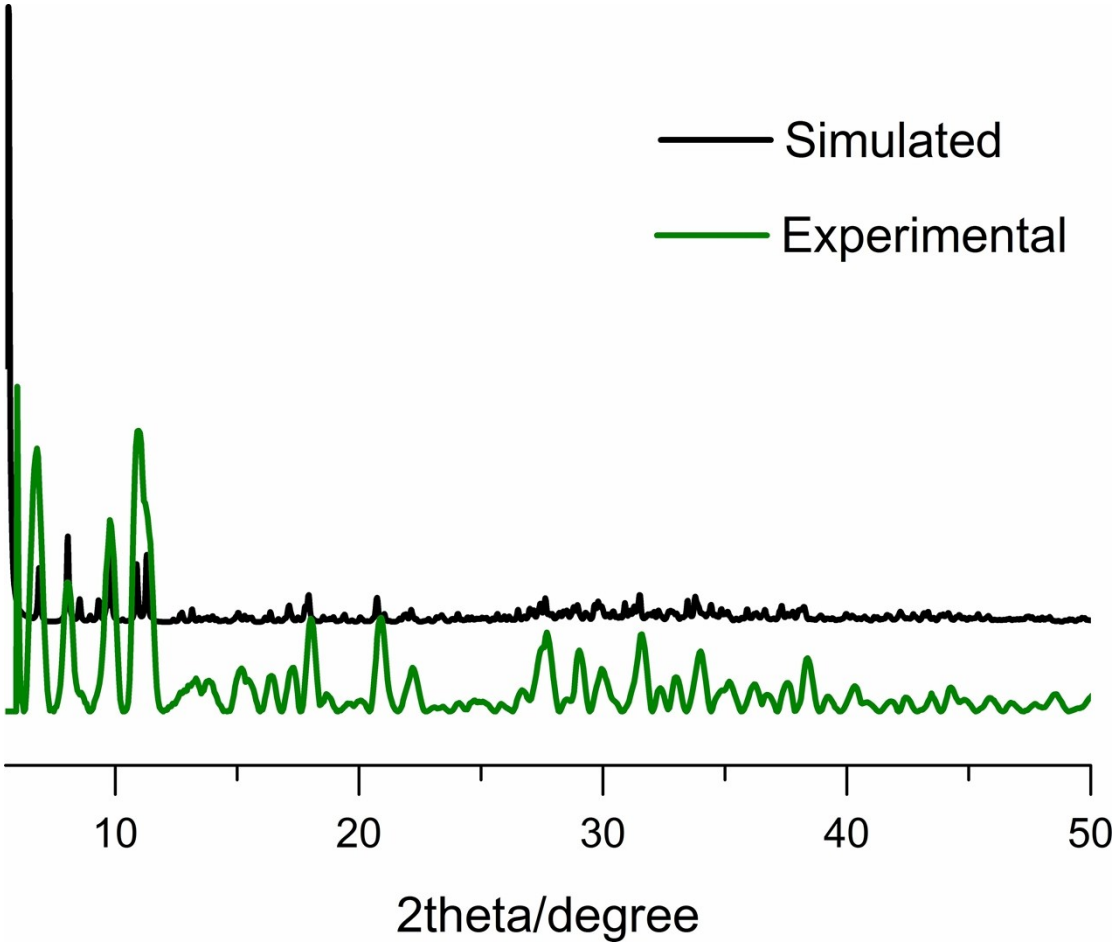

Figure S9: The IR spectrum of SD/Ag44a.

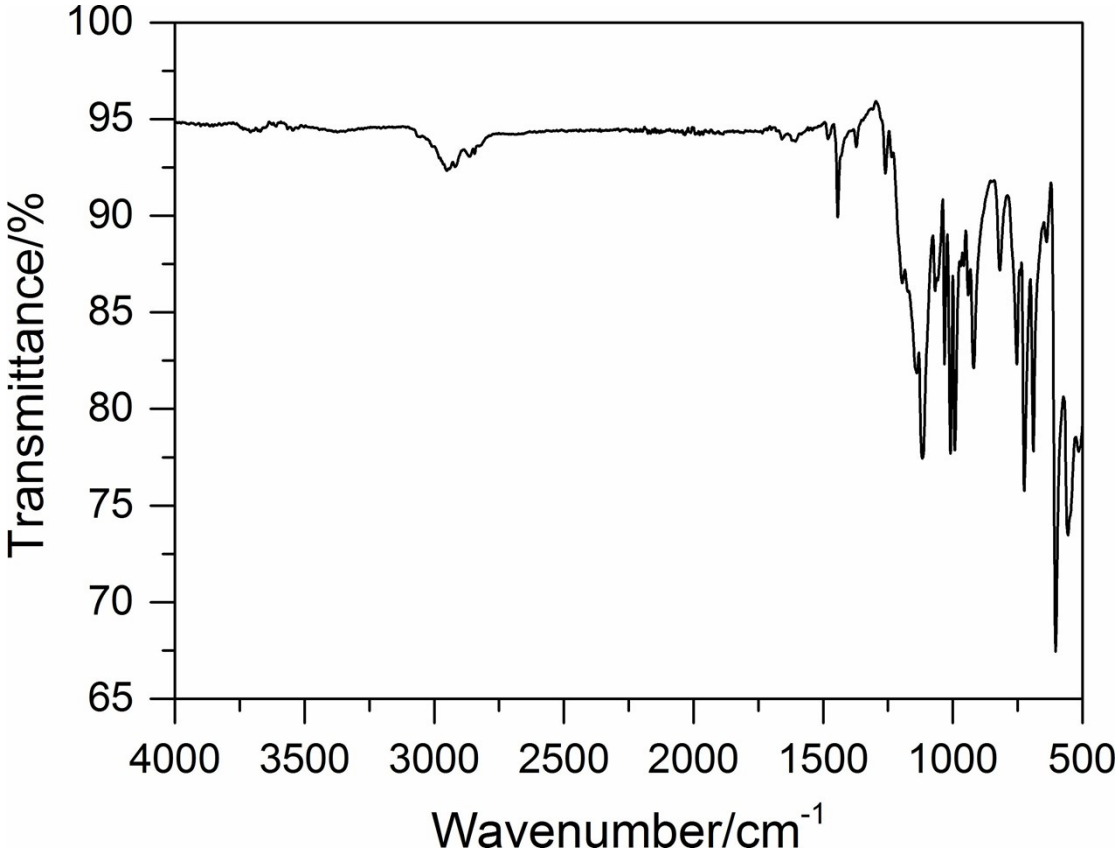

Figure S10: The IR spectrum of SD/Ag46.

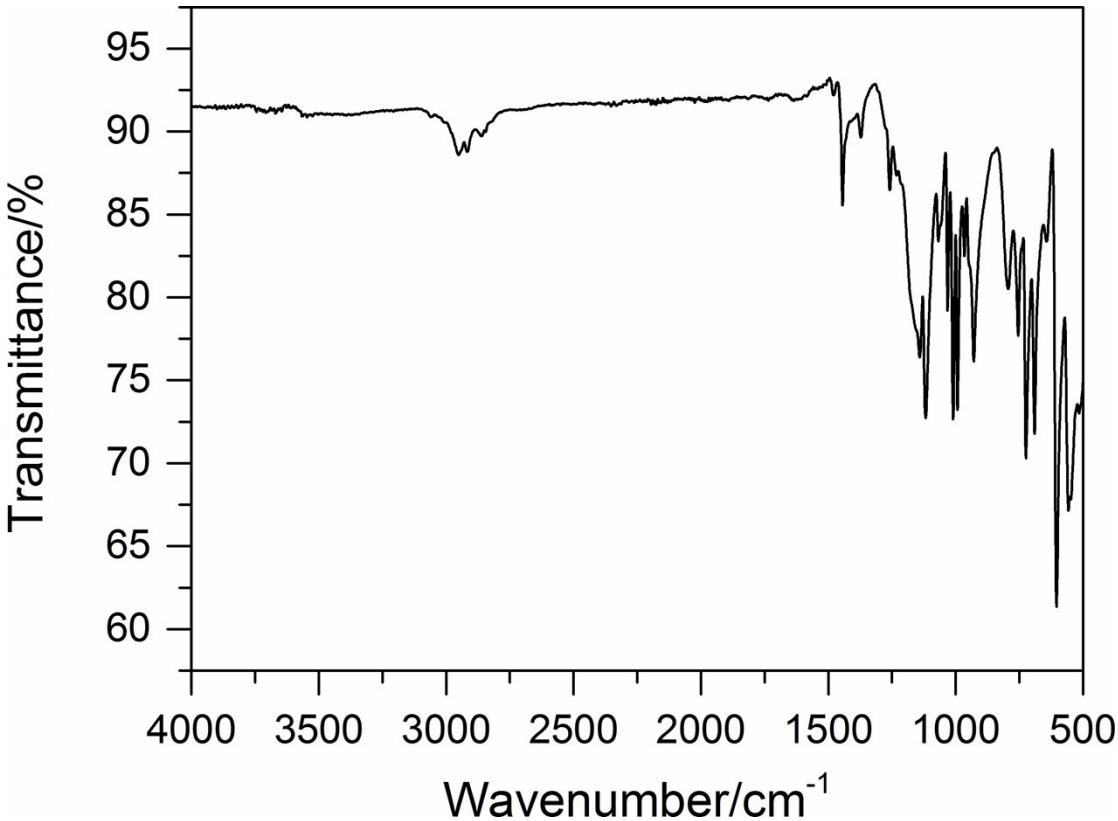

Figure S11: Microscope photographs of crystals SD/Ag44a, SD/Ag46 and SD/Ag44b.

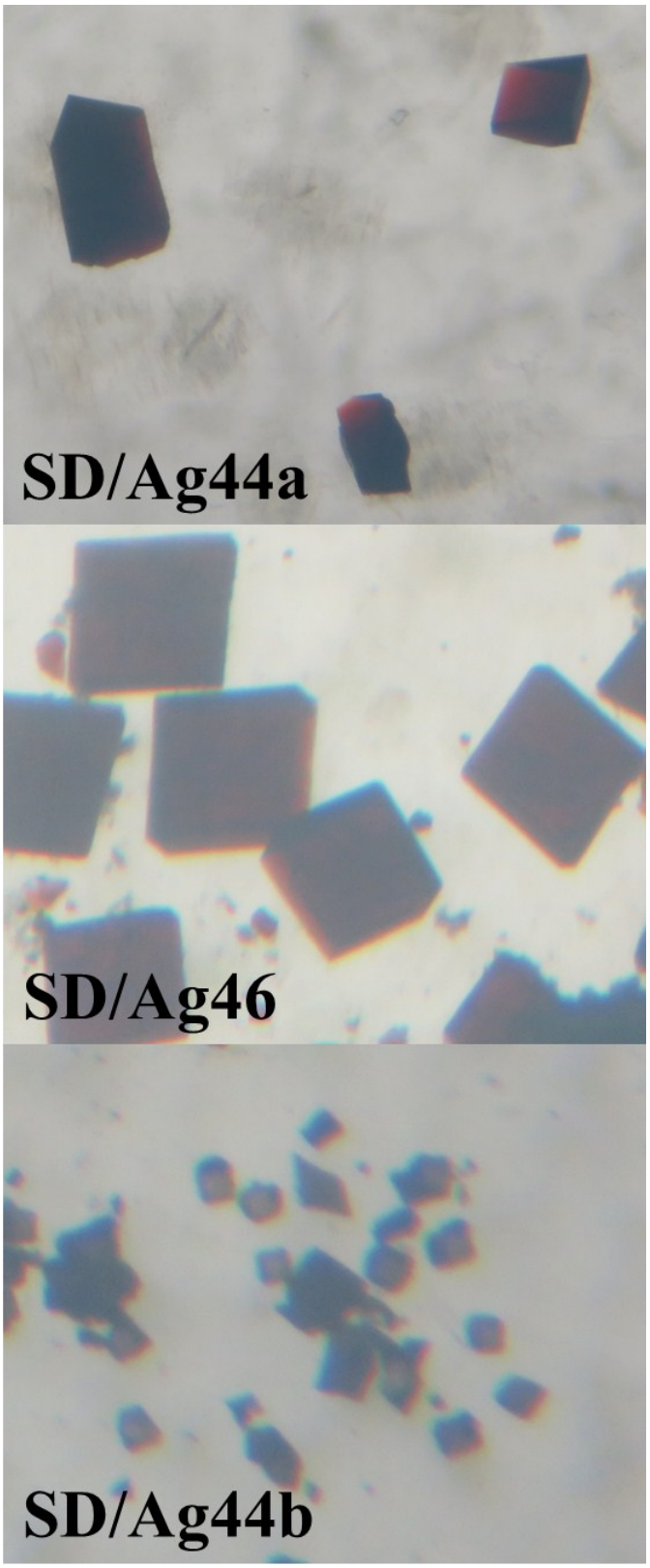

Figure S12: SEM and elemental mapping images of SD/Ag44a.

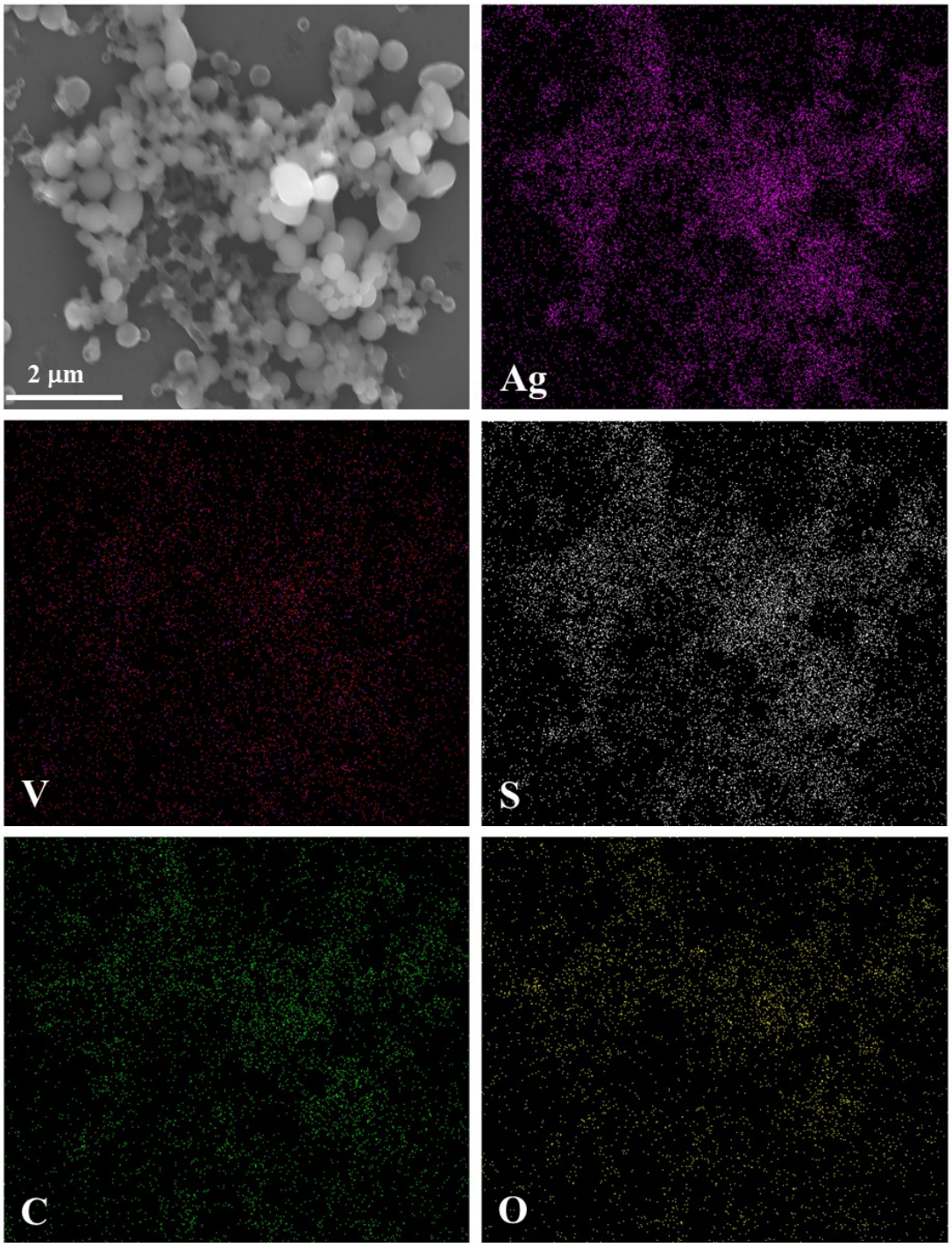

Figure S13: SEM and elemental mapping images of SD/Ag46.

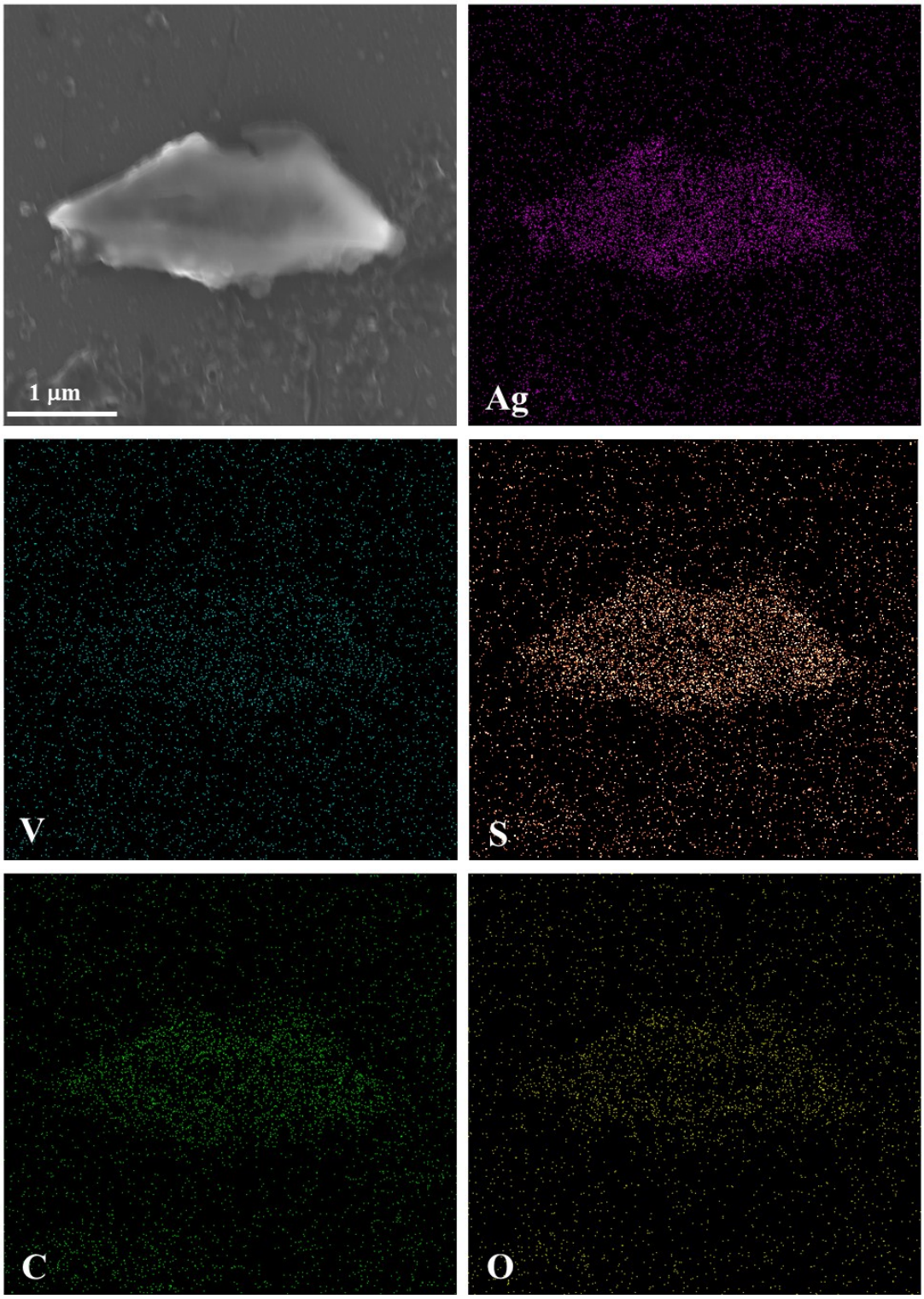

Figure S14: SEM and elemental mapping images of SD/Ag44b.

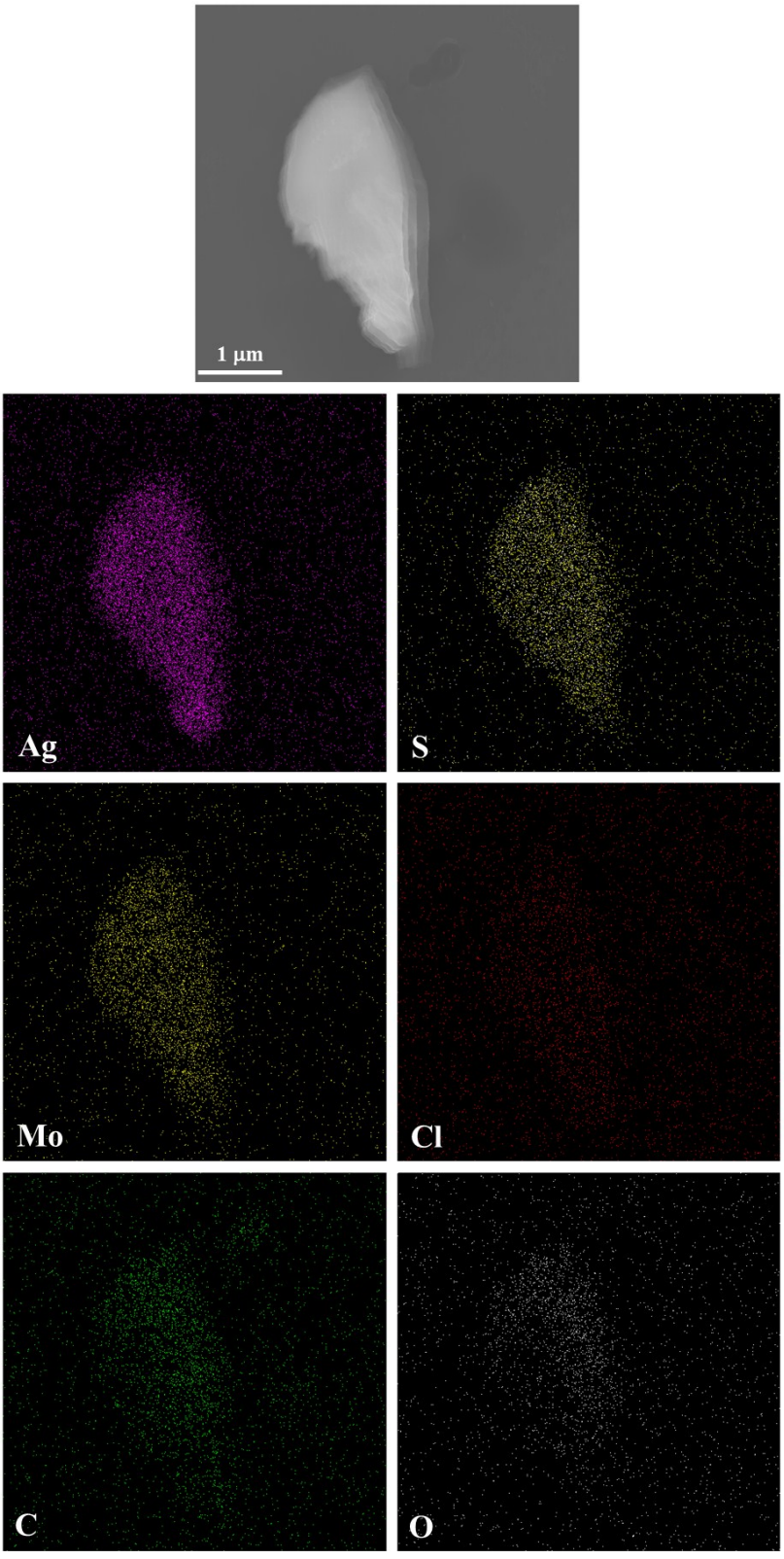

Figure S15: Molecules packing diagrams in 2×2×2 unit cell of SD/Ag44a viewed from different directions.

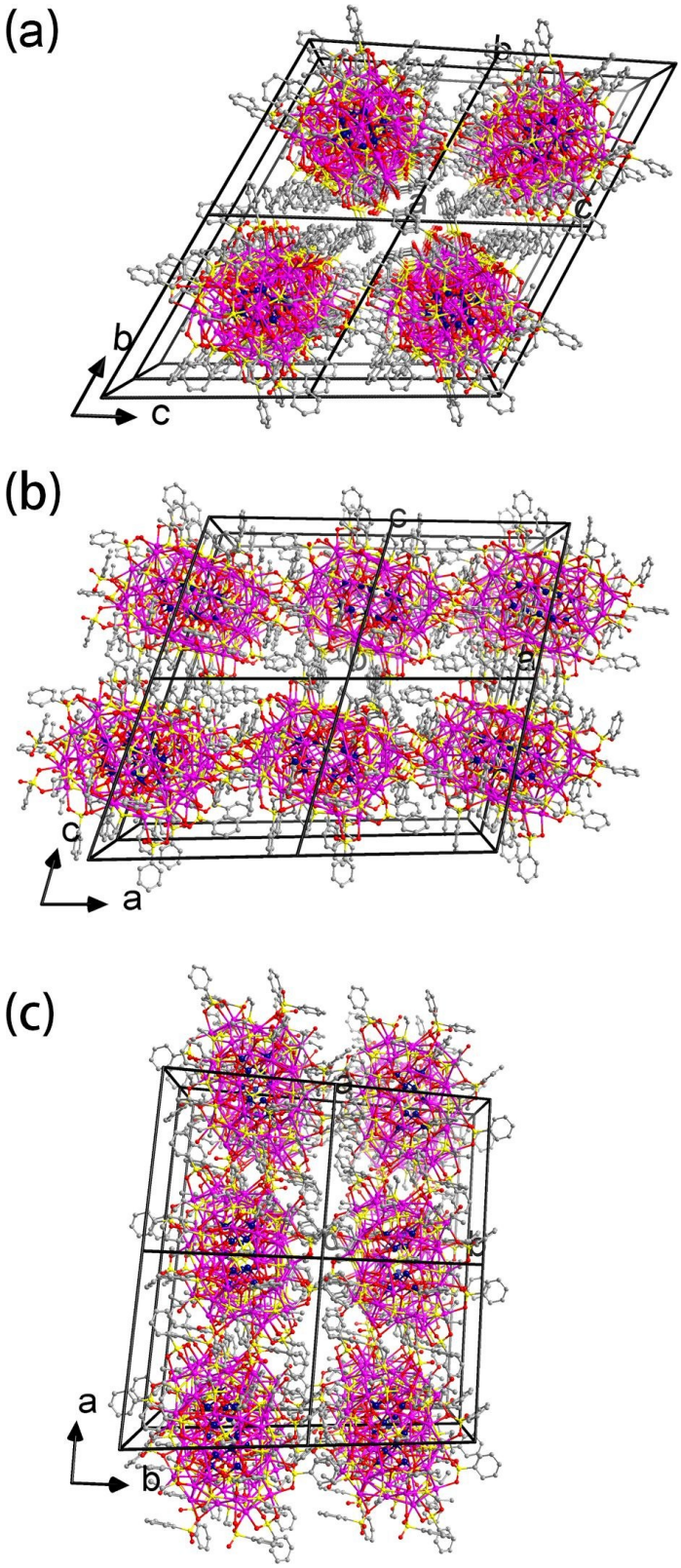

Figure S16: Molecules packing diagrams in 2×2×2 unit cell of SD/Ag46 viewed from different directions.

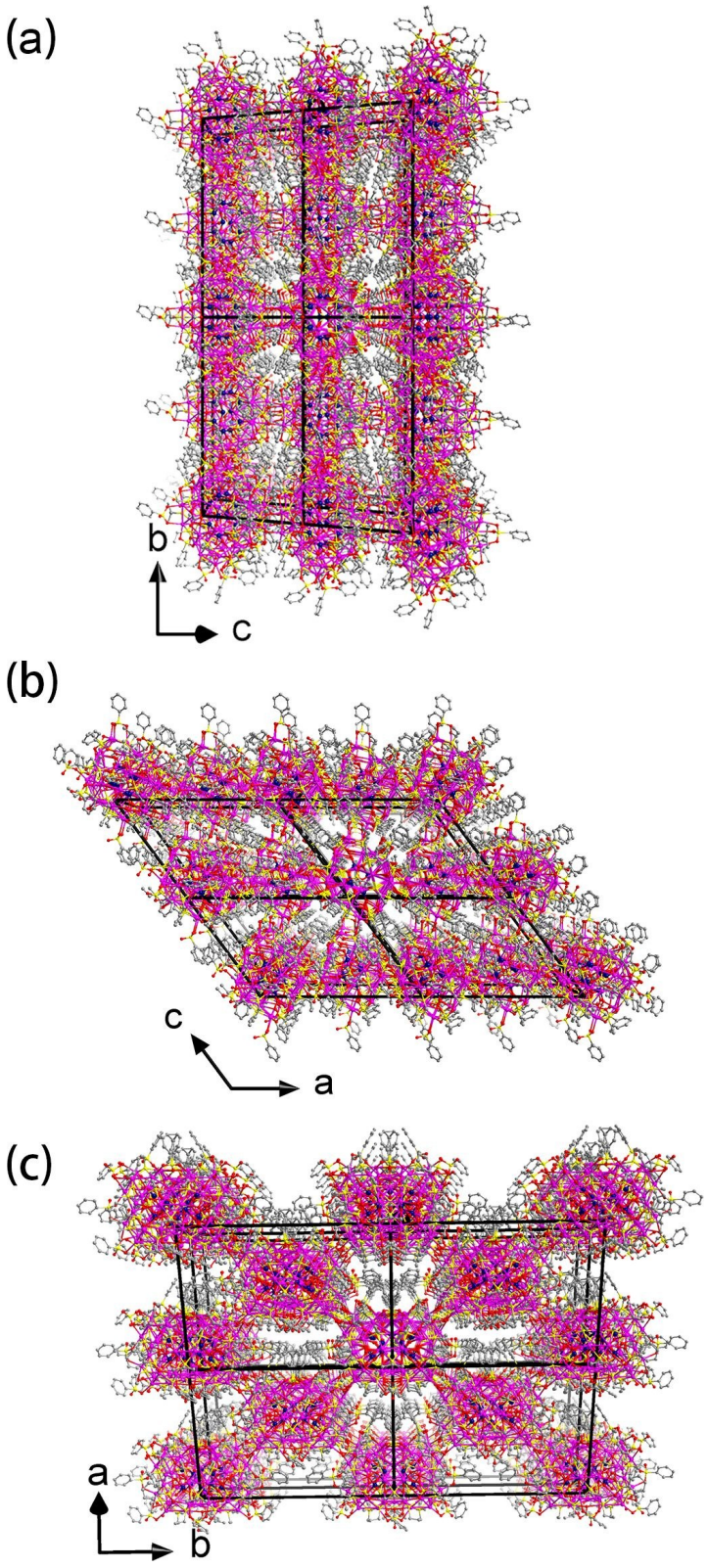

Figure S17: Molecules packing diagrams in 2×2×2 unit cell of SD/Ag44b viewed from different directions.

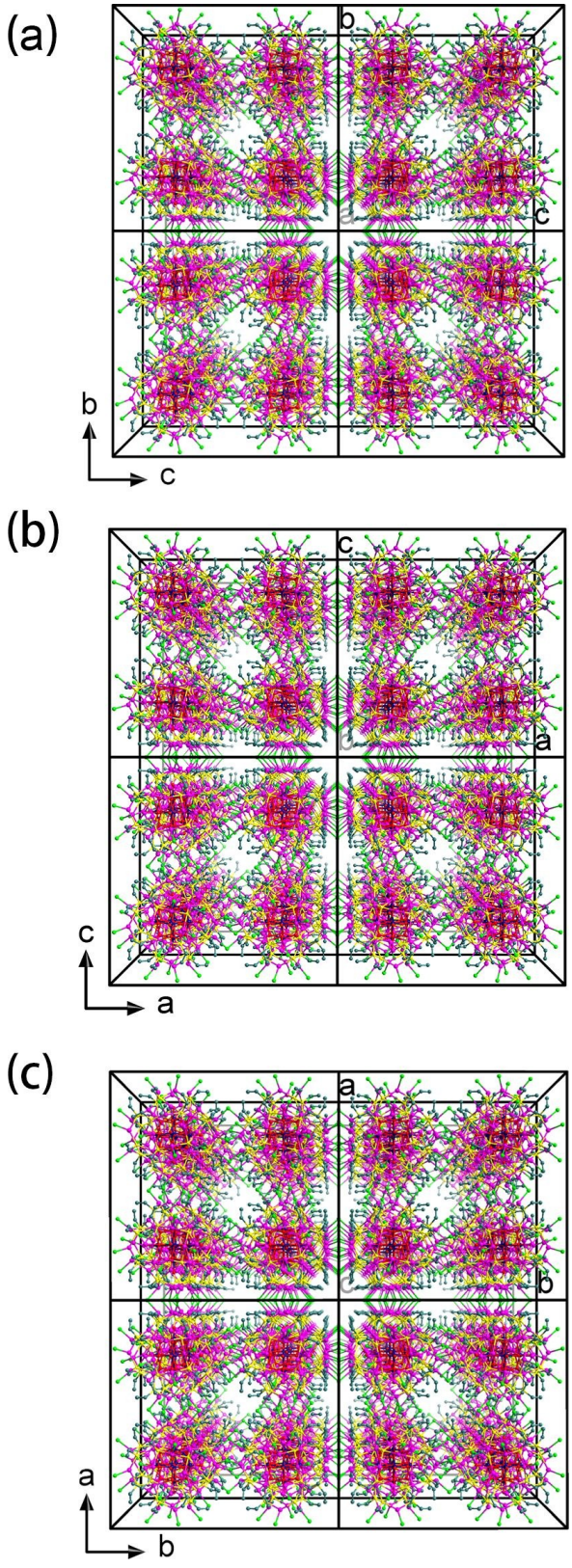

Figure S18: The UV/Vis spectra of SD/Ag46 and $(EtSAg)_n$ precursor.

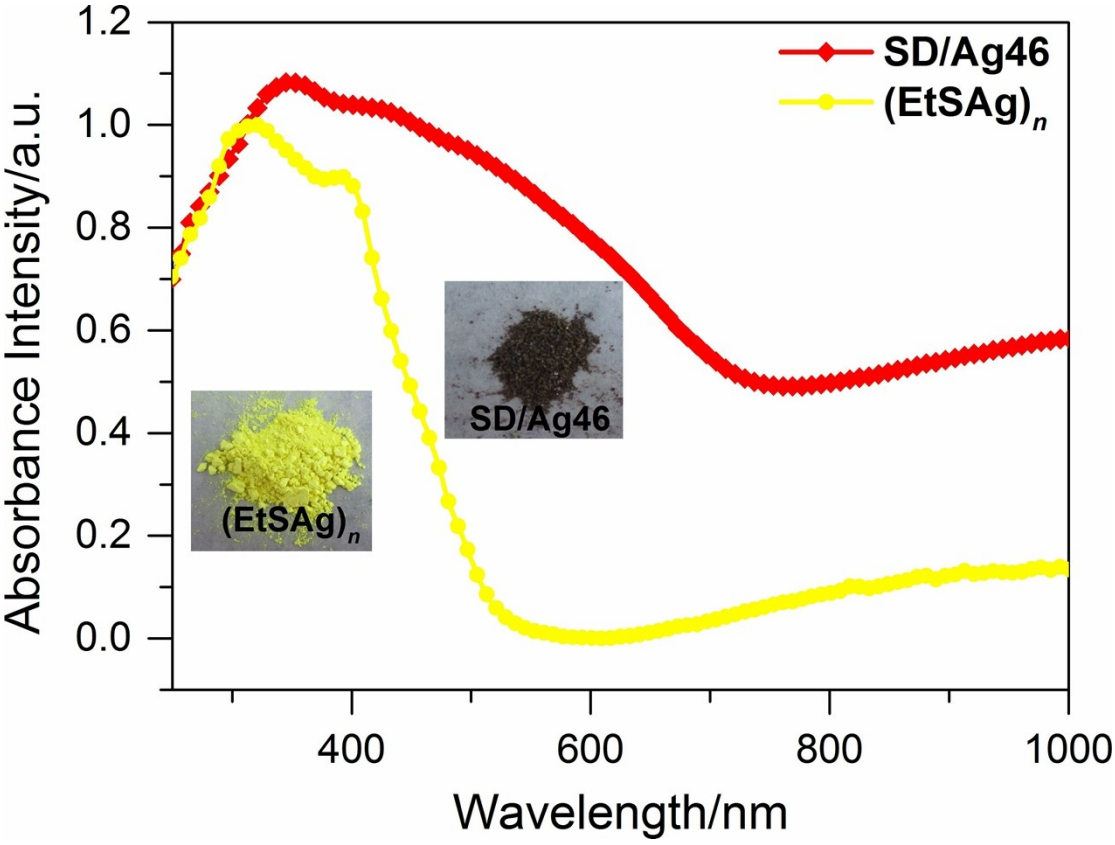

The UV/Vis spectrum of **SD/Ag46** was measured in the solid state at room temperature. As shown in Figure S18, **SD/Ag46** displays two intense absorption peaks, which consist a main peak centered at 325 nm and a shoulder peak at 427 nm tailed to 740 nm. The peak centered at 325 nm can be ascribed to the n→π* transition of EtS^-, as similarly observed in the absorption spectrum of the precursor $(EtSAg)_n$. The visible region (427 nm and its tail) can be assigned to the charge-transfer transition from the S 3p to Ag 5s orbitals. Based on the Kubelka-Munk function (Figure S19), the energy gap of **SD/Ag46** was estimated to be ~0.73 eV, which suggests **SD/Ag46** is a potential narrowband semiconductor. In comparison, the band gap of $(EtSAg)_n$ precursor is ~2.2 eV, which is consistent with the colors of the samples: $(EtSAg)_n$ is yellow, whereas **SD/Ag46** is red.

Figure S19: Adsorption spectra of SD/Ag46 and $(EtSAg)_n$ precursor derived from the diffuse reflectance spectra through Kubelka-Munk function.

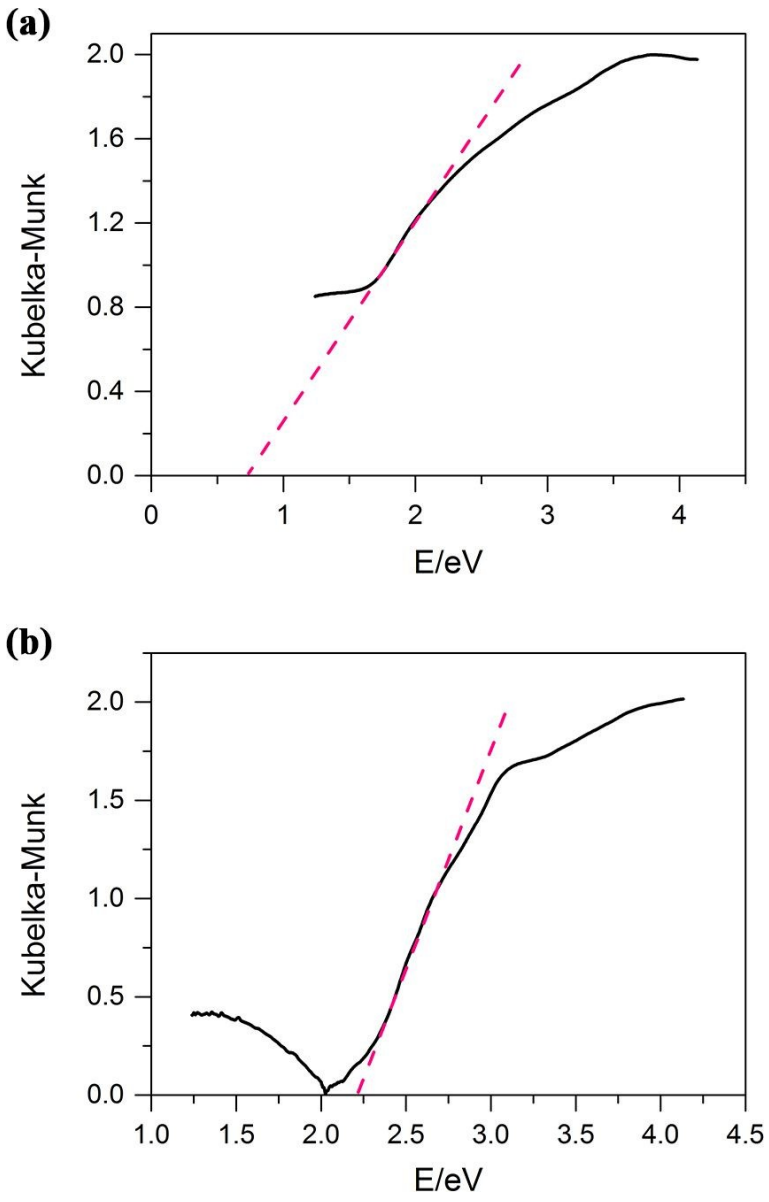

Figure S20: The I/sigma vs. resolution plot of SD/Ag44a derived from reflection data statistics using OLEX 1.2.10.[6]

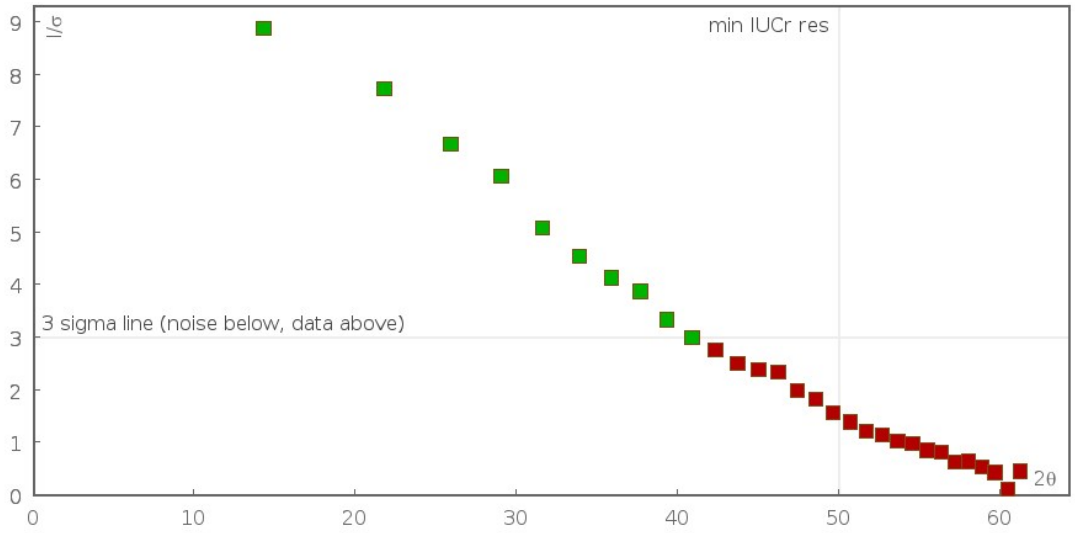

Figure S21: The R_1 factor vs. resolution plot of SD/Ag44a derived from reflection data statistics using OLEX 1.2.10.[6]

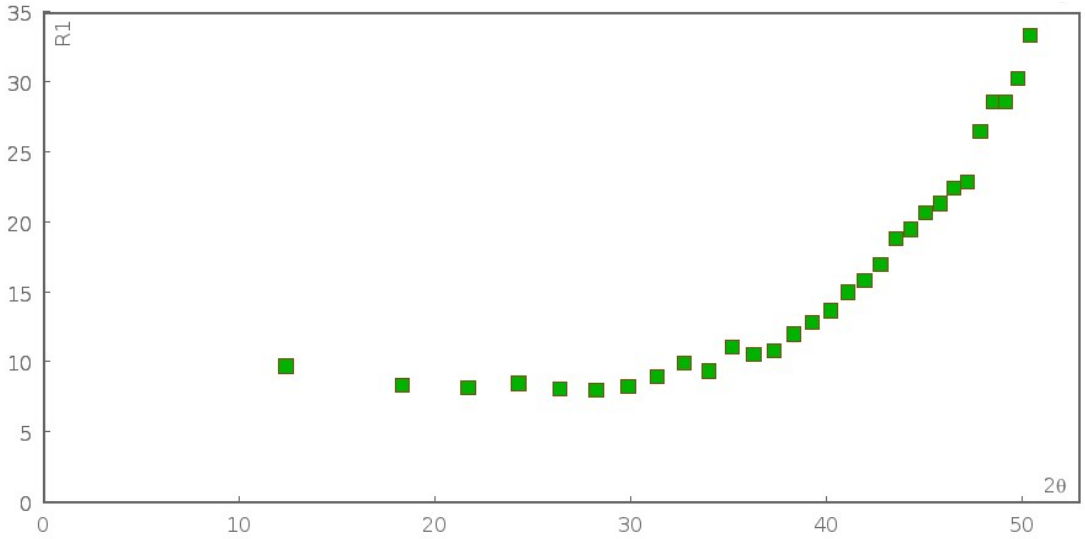

Figure S22: The I/sigma vs. resolution plot of SD/Ag46 derived from reflection data statistics using OLEX 1.2.10.[6]

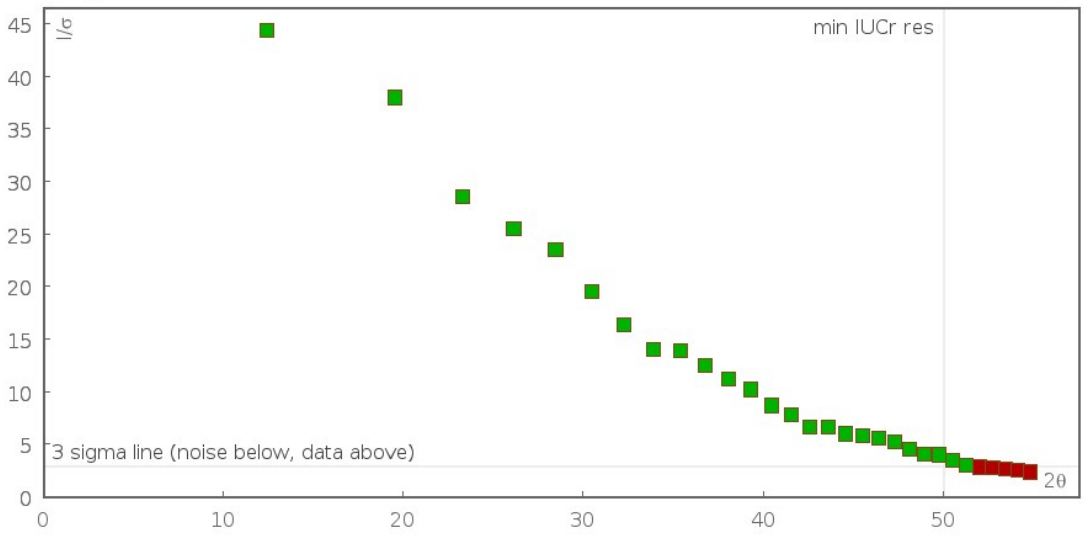

Figure S23: The R_1 factor vs. resolution plot of SD/Ag46 derived from reflection data statistics using OLEX 1.2.10.[6]

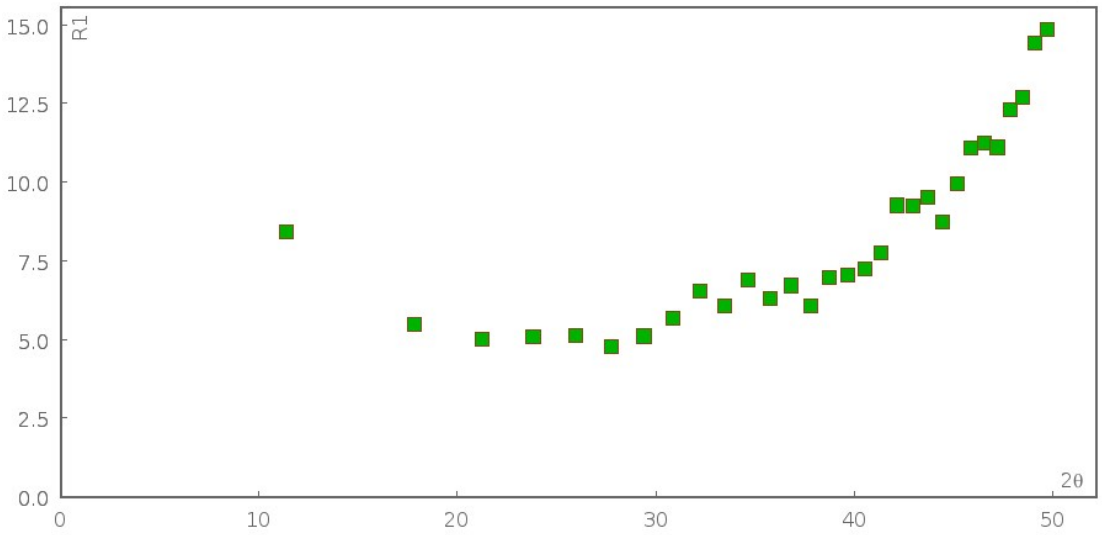

Figure S24: The I/sigma vs. resolution plot of SD/Ag44b derived from reflection data statistics using OLEX 1.2.10.[6]

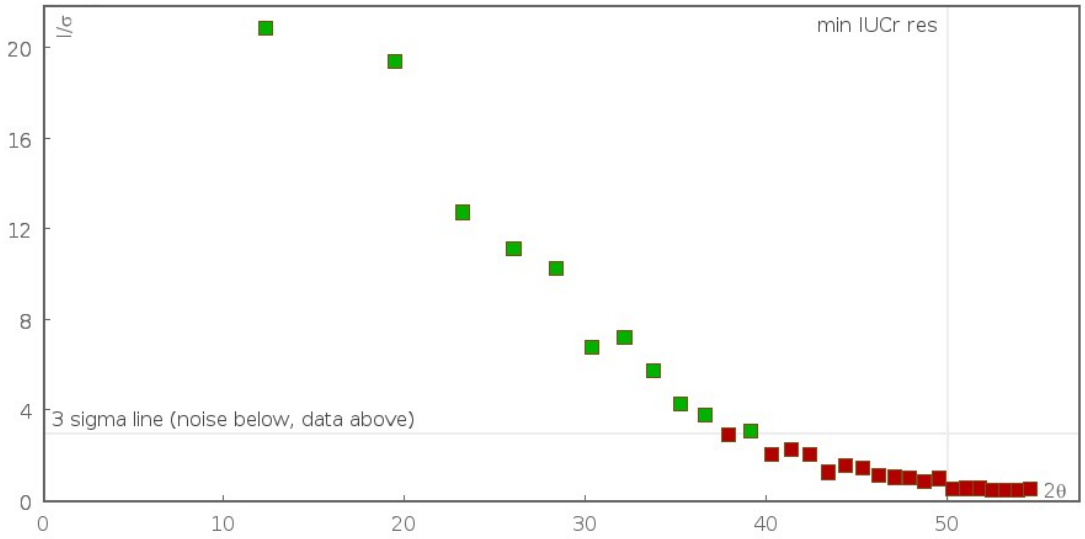

Figure S25: The R_1 factor vs. resolution plot of SD/Ag44b derived from reflection data statistics using OLEX 1.2.10.[6]

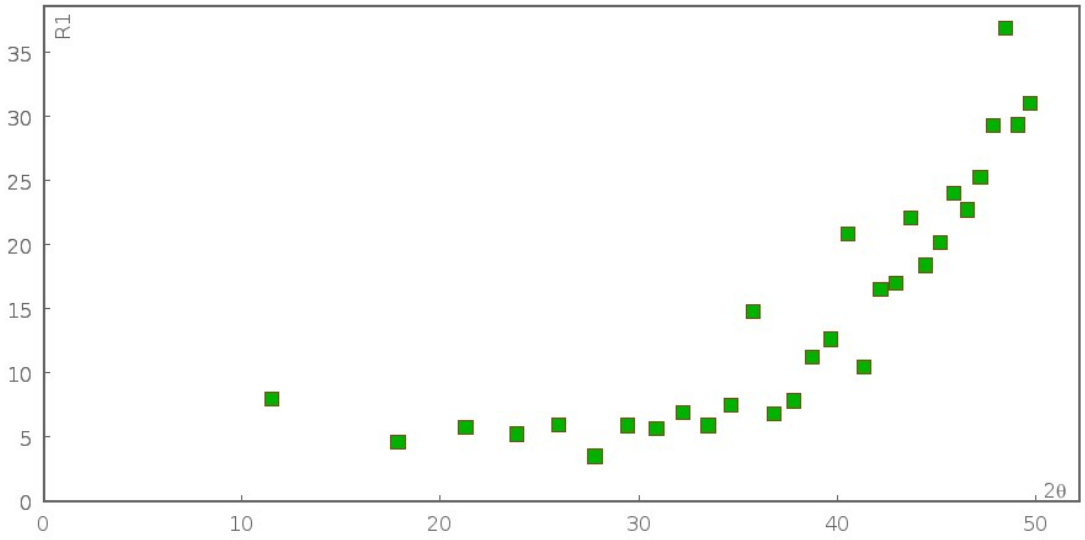

Figure S26: The van der Waals (VDW) surface of SD/Ag44b packing in 2×2×2 unit cell calculated via 3V Volume Assessor program[9] viewed along six different orientations.

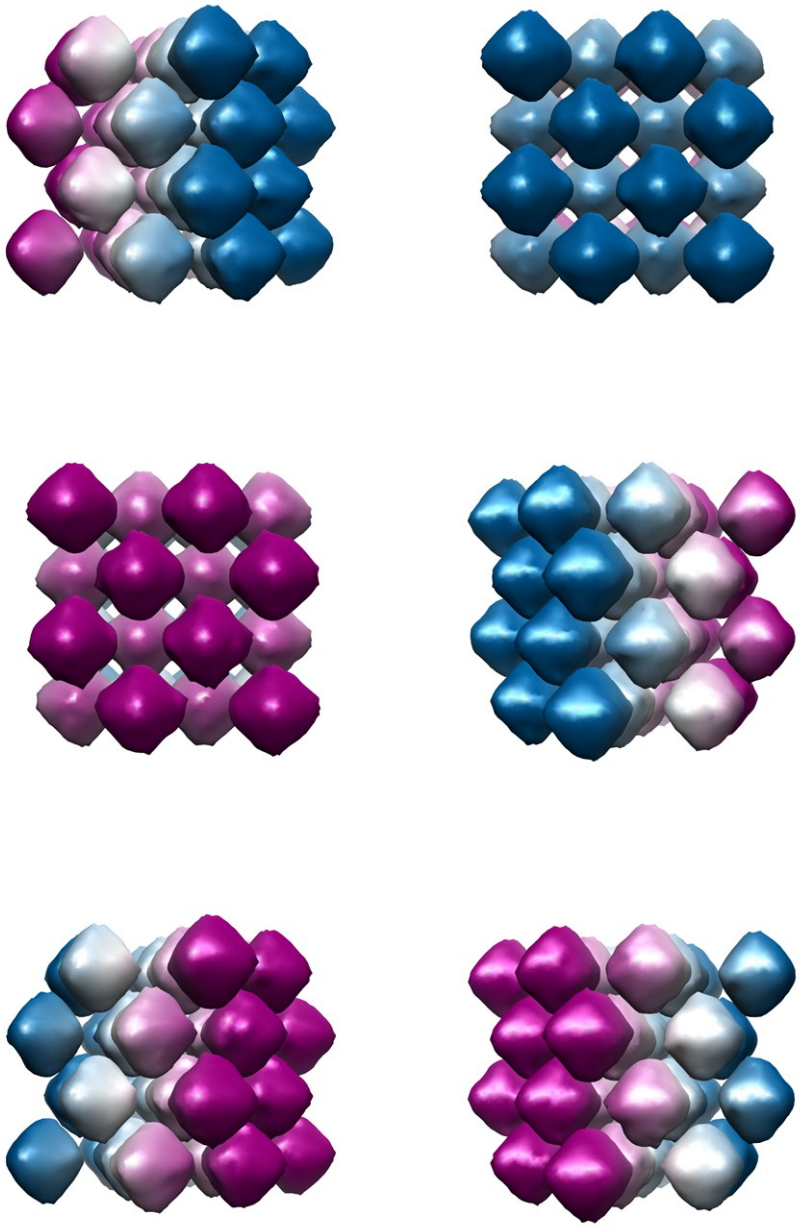

Table S1: Bond valence sum (BVS) calculations for the valences of V in SD/Ag44a, SD/Ag46 and Mo in SD/Ag44b.

SD/Ag44a						
Atoms	V1	V2	V3	V4	V5	
Valence	5.039	5.048	4.959	5.121	4.988	
SD/Ag46						
Atoms	V1	V2	V3	V4	V5	V6
Valence	4.960	4.840	4.943	4.941	4.950	5.002
SD/Ag44b						
Atom	Mo1					
Valence	5.443					

Table S2: Crystal data collection and structure refinement for SD/Ag44a, SD/Ag46 and SD/Ag44b.

Compound	**SD/Ag44a**	**SD/Ag46**	**SD/Ag44b**
Empirical formula	$C_{148}H_{194}Ag_{44}O_{84}S_{38}V_{10}$	$C_{137}H_{190}Ag_{46}O_{76}S_{38}V_{10}$	$C_{48}H_{120}Ag_{44}Cl_{12}Mo_6O_{19}S_{27}$
X-ray diffractometer	Rigaku Oxford Diffraction XtaLAB Synergy	Bruker APEX II	Bruker APEX II
Formula weight	9790.98	9742.58	7614.37
Temperature/K	100.00(10)	123(2)	123(2)
Crystal system	triclinic	monoclinic	cubic
Space group	*P*-1	*Cm*	*Fm*-3*c*
a/Å	19.9658(6)	25.7510(15)	32.558(4)
b/Å	20.2722(14)	30.6808(17)	32.558(4)
c/Å	20.4027(12)	19.5302(11)	32.558(4)
α/°	60.809(7)	90	90
β/°	70.785(4)	126.5766(6)	90
γ/°	78.996(4)	90	90
Volume/Å^3	6803.0(8)	12391.3(12)	34512(13)
Z	1	2	8
ρ_{calc}g/cm^3	2.390	2.611	2.931
μ/mm^{-1}	3.766	4.283	5.822
F(000)	4660.0	9240.0	28128.0
Radiation	MoKα (λ = 0.71073)	MoKα (λ = 0.71073)	MoKα (λ = 0.71073)
Reflections collected	76924	37341	23949
Independent reflections	24752 [R_{int} = 0.1071, R_{sigma} = 0.1061]	17925 [R_{int} = 0.0217, R_{sigma} = 0.0307]	1359 [R_{int} = 0.0737, R_{sigma} = 0.0232]
Data/parameters	24752/1457	17925/1182	1359/66
Goodness-of-fit on F^2	1.024	1.026	1.104
Final R indexes [I>=2σ (I)]	R_1 = 0.0858, wR_2 = 0.2125	R_1 = 0.0591, wR_2 = 0.1593	R_1 = 0.0713, wR_2 = 0.1747
Final R indexes [all data]	R_1 = 0.1256, wR_2 = 0.2387	R_1 = 0.0663, wR_2 = 0.1672	R_1 = 0.1002, wR_2 = 0.2014
Largest diff. peak/hole / e Å^{-3}	4.28/-1.82	4.89/-1.41	3.76/-2.18

Table S3: Selected bond distances (Å) and angles (°) for SD/Ag44a, SD/Ag46 and SD/Ag44b.

SD/Ag44a			
Ag1—Ag2	3.358 (7)	Ag11—O39	2.386 (13)
Ag1—O3	2.525 (11)	Ag11—S6	2.506 (5)
Ag1—S2	2.403 (4)	Ag11—S7	2.501 (4)
Ag1—S9^{i}	2.418 (4)	Ag12—Ag13	3.289 (2)
Ag2—Ag5	3.1094 (17)	Ag12—O1W	2.38 (2)
Ag2—Ag6	3.007 (2)	Ag12—O17	2.489 (13)
Ag2—O22	2.382 (13)	Ag12—S4	2.519 (4)
Ag2—O26	2.496 (10)	Ag12—S7	2.520 (4)
Ag2—S1	2.568 (4)	Ag13—Ag14	3.352 (2)
Ag2—S2	2.520 (4)	Ag13—Ag15	2.9803 (17)
Ag3—Ag7	3.341 (2)	Ag13—O29^{ii}	2.458 (11)
Ag3—Ag18^{i}	2.9890 (19)	Ag13—O41	2.324 (12)
Ag3—Ag19^{i}	3.0462 (19)	Ag13—S4	2.471 (4)
Ag3—S1	2.445 (4)	Ag14—Ag15	3.0392 (18)
Ag3—S10^{i}	2.445 (3)	Ag14—S3	2.384 (4)
Ag4—Ag5	3.0264 (16)	Ag14—S5	2.392 (4)
Ag4—Ag14	3.060 (2)	Ag15—O13	2.483 (8)
Ag4—O28	2.526 (9)	Ag15—S3	2.451 (4)
Ag4—O30	2.449 (12)	Ag15—S4	2.469 (5)
Ag4—S2	2.490 (4)	Ag16—Ag9^{i}	3.215 (2)
Ag4—S3	2.508 (4)	Ag16—O5	2.359 (9)
Ag5—Ag6	2.9857 (16)	Ag16—O32	2.21 (2)
Ag5—Ag14	3.0049 (19)	Ag16—O33	2.378 (15)
Ag5—O25	2.481 (10)	Ag16—S3	2.456 (4)
Ag5—O27	2.485 (9)	Ag17—Ag18	3.2773 (19)
Ag5—S2	2.490 (4)	Ag17—S4	2.491 (3)
Ag5—S5	2.584 (4)	Ag17—S10	2.478 (3)
Ag6—Ag7	2.8829 (15)	Ag18—Ag3^{i}	2.9890 (19)
Ag6—Ag8	3.0259 (19)	Ag18—O1^{i}	2.565 (10)
Ag6—O24	2.440 (11)	Ag18—O6	2.586 (8)
Ag6—S1	2.451 (4)	Ag18—O35	2.60 (2)
Ag6—S5	2.442 (4)	Ag18—O36	2.369 (15)
Ag7—Ag8	3.0433 (18)	Ag18—S10	2.514 (4)
Ag7—O2	2.499 (9)	Ag19—Ag3^{i}	3.0463 (19)
Ag7—O38^{i}	2.537 (11)	Ag19—Ag20	3.1116 (16)
Ag7—S1	2.511 (5)	Ag19—O15	2.409 (16)
Ag7—S6	2.475 (5)	Ag19—O23^{i}	2.515 (13)

Ag8—Ag11	3.0980 (19)	Ag19—S9	2.492 (4)
Ag8—S5	2.482 (4)	Ag19—S10	2.475 (4)
Ag8—S6	2.453 (4)	Ag20—Ag21	3.1782 (16)
Ag9—Ag16^{i}	3.215 (2)	Ag20—Ag22	2.8775 (17)
Ag9—O33^{i}	2.573 (14)	Ag20—O12	2.503 (10)
Ag9—O36^{i}	2.455 (15)	Ag20—O17	2.543 (13)
Ag9—S8	2.489 (5)	Ag20—S7	2.519 (4)
Ag10—Ag22	2.8683 (17)	Ag20—S9	2.510 (3)
Ag10—O18	2.488 (14)	Ag21—Ag22	2.9063 (15)
Ag10—O37^{i}	2.445 (11)	Ag21—O8	2.508 (10)
Ag10—S6	2.528 (3)	Ag21—S8	2.470 (4)
Ag10—S8	2.550 (4)	Ag21—S9	2.471 (4)
Ag11—Ag22	2.8648 (15)	Ag22—S7	2.482 (4)
Ag11—O19	2.538 (13)	Ag22—S8	2.489 (4)
S2—Ag1—O3	79.0 (2)	S7—Ag11—S6	138.16 (14)
S2—Ag1—S9^{i}	165.8 (2)	O1W—Ag12—O17	107.9 (7)
S9^{i}—Ag1—O3	114.7 (2)	O1W—Ag12—S4	103.7 (6)
O22—Ag2—O26	91.7 (4)	O1W—Ag12—S7	110.6 (6)
O22—Ag2—S1	94.3 (4)	O17—Ag12—S4	107.2 (4)
O22—Ag2—S2	114.4 (4)	O17—Ag12—S7	82.9 (3)
O26—Ag2—S1	101.7 (3)	S4—Ag12—S7	139.22 (15)
O26—Ag2—S2	108.2 (3)	O29^{ii}—Ag13—S4	124.6 (3)
S2—Ag2—S1	137.12 (14)	O41—Ag13—O29^{ii}	92.5 (4)
S10^{i}—Ag3—S1	169.30 (14)	O41—Ag13—S4	142.8 (3)
O30—Ag4—O28	84.4 (3)	S3—Ag14—S5	163.95 (16)
O30—Ag4—S2	109.9 (4)	S3—Ag15—O13	106.2 (2)
O30—Ag4—S3	93.3 (4)	S3—Ag15—S4	164.07 (13)
S2—Ag4—O28	102.8 (3)	S4—Ag15—O13	86.0 (2)
S2—Ag4—S3	149.95 (14)	O5—Ag16—O33	81.7 (4)
S3—Ag4—O28	98.1 (3)	O5—Ag16—S3	108.5 (3)
O25—Ag5—O27	87.2 (3)	O32—Ag16—O5	109.1 (5)
O25—Ag5—S2	120.7 (3)	O32—Ag16—O33	101.9 (5)
O25—Ag5—S5	91.0 (3)	O32—Ag16—S3	124.7 (4)
O27—Ag5—S2	110.2 (3)	O33—Ag16—S3	122.5 (4)
O27—Ag5—S5	100.1 (3)	S10—Ag17—S4	150.05 (13)
S2—Ag5—Ag14	107.31 (10)	O1^{i}—Ag18—O6	63.5 (3)
S2—Ag5—S5	136.03 (12)	O1^{i}—Ag18—O35	119.6 (4)
O24—Ag6—S1	95.9 (3)	O6—Ag18—O35	99.3 (4)
O24—Ag6—S5	110.9 (3)	O36—Ag18—O1^{i}	76.6 (4)
S5—Ag6—S1	151.32 (13)	O36—Ag18—O6	135.5 (4)
O2—Ag7—O38^{i}	90.7 (4)	O36—Ag18—O35	83.3 (4)
O2—Ag7—S1	89.0 (2)	O36—Ag18—S10	136.3 (4)
S1—Ag7—O38^{i}	88.6 (3)	S10—Ag18—O1^{i}	141.1 (2)

S6—Ag7—O2	109.3 (2)	S10—Ag18—O6	88.1 (2)
S6—Ag7—O38^{i}	109.1 (3)	S10—Ag18—O35	89.4 (3)
S6—Ag7—S1	153.80 (12)	O15—Ag19—O23^{i}	84.9 (5)
S6—Ag8—S5	148.05 (14)	O15—Ag19—S9	100.5 (5)
O36^{i}—Ag9—O33^{i}	82.6 (5)	O15—Ag19—S10	103.1 (4)
O36^{i}—Ag9—S8	130.9 (3)	S9—Ag19—O23^{i}	88.9 (4)
S8—Ag9—O33^{i}	146.4 (4)	S10—Ag19—O23^{i}	124.8 (4)
O18—Ag10—S6	95.5 (3)	S10—Ag19—S9	140.04 (13)
O18—Ag10—S8	104.8 (3)	O12—Ag20—O17	104.9 (4)
O37^{i}—Ag10—O18	101.1 (4)	O12—Ag20—S7	98.4 (2)
O37^{i}—Ag10—S6	104.0 (3)	O12—Ag20—S9	105.6 (2)
O37^{i}—Ag10—S8	106.0 (3)	S7—Ag20—O17	81.8 (3)
S6—Ag10—S8	139.38 (12)	S9—Ag20—O17	112.7 (3)
O39—Ag11—O19	84.0 (4)	S9—Ag20—S7	146.91 (13)
O39—Ag11—S6	116.8 (5)	S8—Ag21—O8	96.9 (2)
O39—Ag11—S7	100.5 (5)	S8—Ag21—S9	145.67 (15)
S6—Ag11—O19	90.7 (4)	S9—Ag21—O8	107.4 (2)
S7—Ag11—O19	112.4 (4)	S7—Ag22—S8	166.49 (15)
Symmetry codes: (i) −*x*+2, −*y*+1, −*z*+1; (ii) −*x*+1, −*y*+1, −*z*+1.			
SD/Ag46			
Ag1—Ag2	3.042 (3)	Ag13—Ag1^{i}	3.106 (3)
Ag1—Ag13^{i}	3.106 (3)	Ag13—Ag14	3.051 (3)
Ag1—O12	2.590 (14)	Ag13—Ag21	3.122 (3)
Ag1—S2^{i}	2.580 (6)	Ag13—S2	2.483 (6)
Ag1—S3^{i}	2.673 (8)	Ag13—S14	2.525 (6)
Ag2—Ag1^{i}	3.042 (3)	Ag13—O35	2.60 (3)
Ag2—Ag3^{i}	2.925 (3)	Ag14—Ag15	3.117 (3)
Ag2—Ag3	2.925 (3)	Ag14—Ag21	3.133 (3)
Ag2—O13	2.499 (19)	Ag14—Ag23	3.301 (3)
Ag2—S3	2.444 (6)	Ag14—S2	2.517 (6)
Ag2—S3^{i}	2.444 (6)	Ag14—S10	2.451 (7)
Ag3—Ag3^{i}	3.174 (3)	Ag15—Ag16	3.053 (3)
Ag3—Ag4	3.225 (3)	Ag15—Ag23	3.198 (3)
Ag3—O16	2.551 (15)	Ag15—O27^{ii}	2.397 (18)
Ag3—O26	2.569 (16)	Ag15—S2	2.556 (6)
Ag3—S3	2.535 (7)	Ag15—S9	2.604 (7)
Ag3—S4	2.465 (7)	Ag16—O26	2.600 (18)
Ag4—Ag5	2.939 (3)	Ag16—S3	2.457 (6)
Ag4—O23	2.45 (2)	Ag16—S9	2.416 (6)
Ag4—O25	2.400 (16)	Ag17—Ag25	3.199 (3)
Ag4—S4	2.500 (7)	Ag17—O2	2.556 (13)
Ag4—S5	2.514 (6)	Ag17—O24	2.59 (2)
Ag5—Ag4^{i}	2.939 (3)	Ag17—S5	2.483 (6)

Ag5—Ag6^{i}	2.906 (3)	Ag17—S8	2.479 (6)
Ag5—Ag6	2.906 (3)	Ag18—Ag19	3.182 (3)
Ag5—S5^{i}	2.454 (5)	Ag18—Ag24	3.217 (3)
Ag5—S5	2.454 (5)	Ag18—O19	2.39 (3)
Ag6—Ag6^{i}	3.089 (4)	Ag18—O28	2.45 (2)
Ag6—Ag7	3.129 (3)	Ag18—S7	2.614 (6)
Ag6—Ag17	3.104 (3)	Ag18—S8	2.531 (7)
Ag6—S5	2.504 (6)	Ag19—Ag20	3.090 (3)
Ag6—S6	2.481 (6)	Ag19—Ag24	3.211 (3)
Ag7—Ag8	3.098 (2)	Ag19—S7	2.523 (6)
Ag7—S6	2.454 (5)	Ag19—S11	2.526 (7)
Ag7—S7	2.427 (5)	Ag20—O30	2.531 (19)
Ag8—Ag19	3.012 (2)	Ag20—S11	2.442 (6)
Ag8—Ag20	3.023 (3)	Ag20—S12	2.482 (7)
Ag8—S7	2.433 (6)	Ag21—Ag22	3.266 (3)
Ag8—S12	2.442 (6)	Ag21—O8	2.548 (13)
Ag9—Ag10	3.160 (3)	Ag21—O31	2.50 (2)
Ag9—Ag10^{i}	3.160 (3)	Ag21—S10	2.443 (6)
Ag9—O6	2.420 (17)	Ag21—S14	2.424 (7)
Ag9—S12	2.480 (6)	Ag22—Ag23	3.112 (3)
Ag9—S12^{i}	2.480 (6)	Ag22—Ag24	3.329 (3)
Ag10—Ag10^{i}	2.927 (4)	Ag22—O4	2.522 (13)
Ag10—O7	2.496 (14)	Ag22—S10	2.484 (7)
Ag10—O30	2.45 (2)	Ag22—S11	2.448 (8)
Ag10—S12	2.495 (6)	Ag23—O39	2.32 (3)
Ag10—S13	2.466 (6)	Ag23—S9	2.481 (6)
Ag11—Ag11^{i}	3.031 (4)	Ag23—S10	2.452 (6)
Ag11—Ag12	3.072 (3)	Ag24—Ag25	3.026 (3)
Ag11—O33	2.43 (2)	Ag24—O38	2.40 (4)
Ag11—S13	2.522 (6)	Ag24—S8	2.482 (6)
Ag11—S14	2.537 (6)	Ag24—S11	2.507 (6)
Ag12—Ag11^{i}	3.072 (3)	Ag25—O4	2.536 (12)
Ag12—O9	2.437 (19)	Ag25—S8	2.464 (7)
Ag12—S14^{i}	2.441 (6)	Ag25—S9	2.445 (7)
Ag12—S14	2.441 (6)		
O12—Ag1—S3^{i}	93.8 (3)	O27^{ii}—Ag15—S2	108.4 (6)
S2^{i}—Ag1—O12	100.7 (3)	O27^{ii}—Ag15—S9	100.2 (6)
S2^{i}—Ag1—S3^{i}	108.5 (2)	S2—Ag15—S9	135.78 (19)
S3^{i}—Ag2—O13	106.52 (16)	S3—Ag16—O26	86.2 (4)
S3—Ag2—O13	106.53 (16)	S9—Ag16—O26	121.5 (4)
S3—Ag2—S3^{i}	145.8 (3)	S9—Ag16—S3	149.2 (2)
O16—Ag3—O26	96.6 (5)	O2—Ag17—O24	107.3 (6)
S3—Ag3—O16	106.8 (3)	S5—Ag17—O2	94.7 (3)

S3—Ag3—O26	85.3 (4)	S5—Ag17—O24	92.6 (4)
S4—Ag3—O16	88.4 (4)	S8—Ag17—O2	98.2 (3)
S4—Ag3—O26	115.4 (4)	S8—Ag17—O24	102.4 (4)
S4—Ag3—S3	153.2 (2)	S8—Ag17—S5	156.2 (2)
O23—Ag4—S4	97.0 (5)	O19—Ag18—O28	84.0 (8)
O23—Ag4—S5	106.2 (5)	O19—Ag18—S7	94.1 (6)
O25—Ag4—O23	101.0 (6)	O19—Ag18—S8	118.7 (6)
O25—Ag4—S4	116.6 (5)	O28—Ag18—S7	86.3 (5)
O25—Ag4—S5	94.0 (5)	O28—Ag18—S8	120.0 (5)
S4—Ag4—S5	137.2 (2)	S8—Ag18—S7	138.26 (19)
S5^{i}—Ag5—S5	172.9 (3)	S7—Ag19—S11	138.0 (2)
S6—Ag6—S5	146.9 (2)	S11—Ag20—O30	120.4 (6)
S7—Ag7—S6	162.9 (2)	S11—Ag20—S12	159.2 (2)
S7—Ag8—S12	163.9 (2)	S12—Ag20—O30	78.7 (6)
O6—Ag9—S12	110.86 (18)	O31—Ag21—O8	97.8 (6)
O6—Ag9—S12^{i}	110.86 (18)	S10—Ag21—O8	107.0 (3)
S12—Ag9—S12^{i}	130.7 (3)	S10—Ag21—O31	88.1 (5)
O7—Ag10—S12	96.0 (4)	S14—Ag21—O8	82.6 (3)
O30—Ag10—O7	81.4 (6)	S14—Ag21—O31	116.8 (5)
O30—Ag10—S12	80.0 (5)	S14—Ag21—S10	152.4 (2)
O30—Ag10—S13	117.6 (5)	S10—Ag22—O4	116.1 (4)
S13—Ag10—O7	83.7 (4)	S11—Ag22—O4	103.2 (4)
S13—Ag10—S12	162.0 (2)	S11—Ag22—S10	140.6 (2)
O33—Ag11—S13	92.9 (7)	O39—Ag23—S9	94.4 (8)
O33—Ag11—S14	102.1 (7)	O39—Ag23—S10	127.2 (8)
S13—Ag11—S14	154.28 (19)	S10—Ag23—S9	136.56 (18)
O9—Ag12—S14^{i}	110.81 (16)	O38—Ag24—S8	114.6 (8)
O9—Ag12—S14	110.81 (16)	O38—Ag24—S11	90.6 (8)
S14—Ag12—S14^{i}	137.7 (3)	S8—Ag24—S11	140.17 (19)
S2—Ag13—S14	155.0 (2)	S8—Ag25—O4	106.7 (4)
S2—Ag13—O35	98.9 (6)	S9—Ag25—O4	103.5 (4)
S14—Ag13—O35	92.9 (7)	S9—Ag25—S8	149.7 (2)
S10—Ag14—S2	138.8 (2)		
Symmetry codes: (i) *x*, −*y*+1, *z*; (ii) *x*−1/2, −*y*+3/2, *z*.			
SD/Ag44b			
Ag2—Ag3	2.9718 (16)	Ag3—S1	2.9633 (17)
Ag2—Ag1	3.0557 (10)	Ag3—S2^{ii}	2.567 (5)
Ag2—S2	2.444 (5)	Ag1—Ag2^{iii}	3.0557 (10)
Ag3—Ag3^{i}	3.250 (3)	Ag1—S2^{iv}	2.622 (5)
S2—Ag2—S2^{v}	169.4 (2)	S2^{v}—Ag3—Cl1	117.4 (2)
S2—Ag2—O2^{vi}	95.28 (12)	Cl1—Ag3—S1	92.65 (14)
S2^{ii}—Ag3—S1	105.19 (12)	Cl1—Ag3—S2^{ii}	104.3 (2)
S2^{v}—Ag3—S1	106.88 (12)	S2^{v}—Ag1—S2^{iv}	108.80 (13)

S2^{v}—Ag3—S2^{ii}	125.0 (2)		
Symmetry codes: (i) *z*, −*y*+1/2, *x*; (ii) *z*, *x*, *y*; (iii) −*y*+1/2, *x*, *z*; (iv) *y*, *z*, *x*; (v) *y*, −*x*+1/2, *z*; (vi) *x*, −*z*+1/2, *y*; (vii) *z*, −*x*+1/2, −*y*+1/2; (viii) −*y*+1/2, −*z*+1/2, *x*.			

References

1. Z. Wang, H. F. Su, X. P. Wang, Q. Q. Zhao, C. H. Tung, D. Sun and L. S. Zheng, *Chem. Eur. J.* 2018, **24**, 1640.
2. Rigaku Oxford Diffraction. *CrysAlis^{Pro} Software system, version 1.171.40.25a*, Rigaku Corporation: Oxford, UK, 2018.
3. *APEX2*, *SAINT* and *SADABS*. Bruker AXS Inc., Madison, Wisconsin, USA, 2008.
4. L. Palatinus and G. Chapuis, *J. Appl. Crystallogr.* 2007, **40**, 786.
5. G. M. Sheldrick, *Acta. Crystallogr., Sect. C* 2015, **71**, 3.
6. O. V. Dolomanov, L. J. Bourhis, R. J. Gildea, J. A. K. Howard, H. Puschmann, *J. Appl. Crystallogr.* 2009, **42**, 339.
7. A. L. Spek, *Acta. Crystallogr., Sect. D*. 2009, **65**, 148.
8. G. G. Gao, P. S. Cheng, T. C. W. Mak, *J Am Chem Soc* 2009, **131**, 18257.
9. N. R. Voss, M. Gerstein, *Nucleic Acids Res* 2010, **38**, W555.